

# Towards observation of three-nucleon short-range correlations in high $Q^2$ $A(e, e')X$ reactions

Donal B. Day<sup>1</sup>, Leonid L. Frankfurt<sup>2</sup>, Misak M. Sargsian<sup>3</sup> and Mark I. Strikman<sup>4</sup>

<sup>1</sup> *Department of Physics, University of Virginia, Charlottesville, VA 22904*

<sup>2</sup> *Sackler School of Exact Sciences, Tel Aviv University, Tel Aviv, Israel*

<sup>3</sup> *Department of Physics, Florida International University, Miami, FL 33199*

<sup>4</sup> *Department of Physics, Pennsylvania State University, University Park, PA*

(Dated: March 6, 2024)

## Abstract

We present a detailed study of kinematical and dynamical conditions necessary for probing highly elusive three-nucleon short range correlations (3N-SRCs) in nuclei through inclusive electron scattering. The kinematic requirements that should be satisfied in order to isolate 3N-SRCs in inclusive processes are derived. We demonstrate that a sequence of two short-range NN interactions represents the main mechanism for 3N-SRCs in inclusive processes. Within this mechanism we predict a quadratic dependence of the inclusive cross section ratios of nuclei to  ${}^3\text{He}$  in the 3N-SRC region to the same ratio measured in 2N-SRC domain. The extended analysis of the available data satisfying the necessary 3N-SRC kinematical conditions is presented. This analysis provides tantalizing signatures of scaling associated with the onset of 3N-SRC dominance. The same data are also consistent with the prediction of the quadratic relation between the ratios measured in the 3N and 2N-SRC regions for nuclei ranging  $4 \leq A \leq 197$ . This agreement made it possible to extract  $a_3(A)$ , the probability of 3N-SRCs relative to the  $A=3$  nucleus. We find  $a_3(A)$  to be significantly larger in magnitude than the analogous parameter,  $a_2(A)$ , for 2N-SRCs.

## I. INTRODUCTION

For the last several decades there have been intensive studies of two-nucleon short range correlations (SRCs) in nuclei utilizing large energy transfer nuclear reactions involving both electron[1–7] and proton[8, 9] probes. Inclusive electron scattering experiments[2, 3, 6], in which only the scattered electron is detected, established the existence of the scaling properties associated with 2N-SRCs, confirming the observation[1] based on the analysis of SLAC data[10–15]. From these experiments  $a_2(A, Z)$ , describing the probability of finding 2N-SRC in a given nucleus relative to the deuteron, was extracted. The analysis of  $A(p, 2p)X$  data yielded similar estimates for  $a_2(A, Z)$  for proton induced reactions[16]. Moreover, the strength of 2N-SRCs found in these analyses agreed with the one obtained from fast backward nucleon production in high energy inclusive  $p(\gamma) - A$  scattering [17]. The consistency among these measurements of the 2N-SRC strength with different probes supports the notion that a genuine property of the nuclear ground state wave function has been probed.

The extension of 2N-SRC studies to semi-inclusive processes in which, in addition to the scattered probe, the struck nucleons[4, 5] or both struck and recoil nucleons from 2N-SRCs[8, 9] have been detected, discovered the strong (a factor of 20) dominance[5, 18] of  $pn$  SRCs as compared to  $pp$  and  $nn$  SRCs in the probed internal momentum range of 300 – 650 MeV/c. The  $pn$  excess is understood[19, 20] when considering the dominance of the tensor interaction at inter-nucleon distances of 0.8 – 1.2 fm and which supports the notion of the commanding role of 2N-SRCs in the high momentum component of the nuclear wave function. Based on the  $pn$ -SRC dominance it was predicted that small component in asymmetric nuclei should have larger kinetics energy[21] which was confirmed experimentally[22–24].

The experimental focus on 2N-SRCs stimulated extensive theoretical efforts (see e.g. Refs.[17, 25–29]) to calculate the multitude of nuclear quantities entering into the cross sections of inclusive and semi-inclusive electron nuclear scattering. Such quantities are the nuclear spectral and decay functions which were calculated based on the 2N-SRC model of high momentum component of the nuclear ground state wave function.

A question which naturally arises is what is the structure of nuclear wave function at even larger internal momenta of the bound nucleons ( $> 650$  MeV/c). One of the important issues in this regard is the possible formation of 3N-SRCs. Understanding the strength and dynamics of 3N-SRCs is essential to advance our knowledge of super-dense nuclear matter.

In most realistic models of the nuclear equation of state 3N-SRCs play an increasingly important role above the saturation densities (see e.g. Ref.[30]).

Experimental evidence for 3N-SRCs is very limited. One of the main obstacles in isolating and probing 3N-SRCs is that they have a much reduced probability compared to 2N-SRCs. As follows from the analysis of Lippmann-Schwinger type equations for nuclear bound states[31, 32], it is likely that 2N-SRCs dominate the momentum distribution for momenta larger than those characteristic of 2N-SRCs. Thus the study of 3N-SRCs requires the consideration of variables other than just the momentum of the bound nucleon. One such parameter is  $\alpha$  [17] which is the light-cone (LC) momentum fraction of the nucleus carried by the bound nucleon. In collider kinematics  $\alpha$  is equal to the ratio of the nucleon longitudinal momentum to the nucleus momentum, scaled by  $A$ ; such that in the case of equal partition of the nuclear momentum,  $\alpha = 1$ . The condition that  $\alpha > 2$  requires at least three nucleons to be in close proximity in order for a single nucleon to carry more than two nucleon's momentum fraction. An early analysis of few nucleon SRCs[17] in the backward production of protons with momenta  $0.3 < p < 1.5$  GeV/c indicated that the scattering off 3N-SRCs begins to dominate the 2N-SRC contribution starting at  $\alpha \simeq 1.6$ , which we consider as a kinematic threshold for isolating 3N-SRCs.

In inclusive  $A(e,e')X$  reactions it is expected that the dominance of 3N-SRCs will be revealed by the onset of another plateau in the ratios of per-nucleon cross sections of heavy to light nuclei at  $x > 2$ . However observation of such a plateau has been elusive. One of the first attempts to isolate 3N-SRC at Bjorken  $x > 2$  observed a possible plateau[3], though subsequent measurements of the ratio  $\frac{3\sigma_{4He}}{4\sigma_{3He}}$  did not make that claim [6]. The most recent measurement[33] of the inclusive cross section ratios of  $^4\text{He}$  to  $^3\text{He}$  at  $x > 2$  and  $1.5 < Q^2 < 1.9$  GeV<sup>2</sup> are largely in agreement with Ref. [6] in that no plateau was observed. This situation corroborated the suggestion[34] that poor momentum resolution for the scattered electrons in the experiment of Ref.[3] allowed events to migrate from smaller to larger  $x$  bins and was responsible for the appearance of the plateau at  $x > 2$ .

In the recent work[35] we reported the partial analysis of inclusive  $A(e,e')X$  data utilizing the above discussed kinematic variable  $\alpha$  for ( $\gtrsim 1.6$ ) region. We demonstrated that the data in this domain show a tantalizing signature for another layer of scaling for the ratio of per-nucleon inclusive cross sections  $\frac{3\sigma(^4He)}{4\sigma(^3He)}$ . The analysis of other nuclei indicated also an agreement with the theoretical prediction of a quadratic proportionality of  $a_3(A)$  to the ratio

of  $\frac{a_2(A)}{a_2(A=3)}$  measured in the 2N SRC domain.

In the current paper we present a detailed theoretical analysis of inclusive scattering at  $\alpha > 1$  kinematics and provide a theoretical foundation for the possibility of observation of new layer of nuclear scaling at  $\alpha > \alpha_{3N}^0$  as well as the expectation of a quadratic proportionality between the probabilities of 2N- and 3N- SRCs in nuclei. We also present a more complete analysis of the experimental data of Ref.[6, 36] using varied approaches to treat the poor quality of the cross section at large  $x$ , expected to be dominated by 3N SRCs.

In Sec. II we elaborate on the kinematics of 3N-SRCs using the variable  $\alpha$  that characterizes the light-cone momentum fraction of the nucleus carried by the bound nucleon. By analyzing the decay function of the  $^3\text{He}$  nucleus we identify the dominating mechanism of 3N-SRCs in inclusive  $eA$  scattering and within this picture calculate the LC momentum fraction,  $\alpha_{3N}$  corresponding to the scattering from a nucleon in 3N-SRC. This variable allows us to identify the kinematics most optimal for probing 3N-SRCs in inclusive scattering. Sec. III discusses the dynamical origin of 3N-SRCs. Based on the model in which 3N-SRCs are generated through the two successive  $pn$  short range interactions it is predicted that the light-cone nuclear density matrix which enters in  $A(e, e')X$  cross section is proportional to the convolution of two  $pn$ -SRC density functions. In Sec. IV final state interactions in inclusive processes are considered as a potential source of destroying or masquerading 3N SRCs. Here we employ the important property of high energy small angle scattering where the quantity  $\alpha$  is approximately conserved in rescattering processes. An experimental observable of 3N-SRCs in  $A(e, e')X$  reactions is presented in Sec. V, where we also derive the quadratic relation between the ratios of inclusive cross sections measured in the 3N- and 2N SRC regions. Sec. VI presents the analysis of the existing inclusive data in light of the theoretical considerations presented in the previous sections. In Sec. VII we summarize our results and give an outlook on the perspective of unambiguous verification of 3N SRCs.

## II. DEFINITION OF 2N AND 3N SRCS

In a non-relativistic formulation we define a nucleon to be in a 2N SRC pair if its momentum exceeds the characteristic nuclear Fermi momentum, ( $k_F \sim 250 \text{ MeV}/c$ ) and is almost completely balanced by the momentum of the correlated nucleon in the pair. In the light-cone representation the requirement is that LC momentum fractions of the correlated

nucleons  $\alpha_1$  and  $\alpha_2$  satisfy conditions:  $\alpha_i \geq 1.3$  or  $\alpha_i \leq 0.7$  for  $i = 1, 2$  and  $\alpha_1 + \alpha_2 \approx 2$ . There are also 2N-SRCs with  $\alpha_i \sim 1$  and  $p_\perp > 0.3$  GeV/c, however they are not important for inclusive scattering at  $x > 1$ .

For the nucleon in a 3N SRC we assume again, that its momentum significantly exceeds  $k_F$ , but in this case this momentum is balanced by two correlated nucleons each with momenta exceeding  $k_F$ . As in the case of 2N SRC the center of mass momentum of the 3N SRC is small,  $p_{cm} \leq k_F$ . The description of 3N-SRCs in the LF representation corresponds to the situation in which  $\alpha_i \geq 1.3$  or  $\alpha_i \leq 0.7$  for  $i = 1, 2, 3$  and  $\alpha_1 + \alpha_2 + \alpha_3 \approx 3$ . Similar to 2N-SRC case, some 3N correlations may correspond to the kinematics in which  $\alpha_i \sim 1$  with nucleons having very large transverse momenta. We do not discuss here such correlations since they contribute very little to  $A(e, e')X$  reactions at  $x > 1$ .

The complete nuclear wave function should incorporate components related to 2N- and 3N-SRCs. However, the first principle calculation of a wave function containing these components is currently impossible due to a poor understanding of strong interaction dynamics at short internucleon distances. Relativistic effects that become increasingly important at large momenta of nucleons involved in short range correlations are also an impediment.

In this respect the progress can be achieved by experimental studies of 3N-SRCs which are currently becoming more accessible with the 12 GeV energy upgrade of Jefferson Lab. One way of addressing the problem of experimentally isolating 3N-SRCs, is a proper identification of the experimentally determined variables that can unambiguously discriminate 3N- from 2N- SRCs. As was mentioned in the introduction, the relevant variable is the light-cone momentum fraction of the nucleus carried by the interacting bound nucleon,  $\alpha$ , first suggested in Ref.[17, 37]. The  $\alpha$  variable, in the reference frame in which nucleus has a large momentum in  $-z$  direction, is defined as [59]:

$$\alpha = A \frac{E_N - k_{N,z}}{E_A - k_{A,z}}, \quad (1)$$

where  $(E_A, k_{A,z})$  and  $(E_N, k_{N,z})$  are the energy and longitudinal momentum of the nucleus and bound nucleon respectively in the noncovariant LF nuclear wave function.

It was first suggested in Ref.[17] that, due to the short-range nature of nuclear forces, when

$$j - 1 < \alpha < j, \quad (2)$$

where  $j > 2$ , the scattering from  $j$ -nucleon SRC from the nucleus will be ensured. However,

the fact that the probability of a  $j$ -nucleon SRC in finite nuclei is  $\sim (\frac{r_{NN}}{r_{AV}})^{3(j-1)}$  with a correlation length  $r_{NN} \ll r_{AV}$ , where  $r_{AV}$  is the average internucleon distance, suggests that the transition from  $j$  to the  $j+1$  SRC should occur at somewhat smaller  $\alpha \lesssim j$  [17]. The latter means that 3N SRCs begin to dominate at  $\alpha \simeq 2$ .

### A. 2N SRCs

In 1993, guided by Eq.(2), we studied the possibility of exposing 2N- SRCs in high  $Q^2$  inclusive  $A(e, e')X$  reactions[1] by identifying the relevant light-cone momentum fraction  $\alpha_{2N}$  for inclusive processes as:

$$\alpha_{2N} = 2 - \frac{q_- + 2m_N}{2m_N} \left( 1 + \frac{\sqrt{W_{2N}^2 - 4m_N^2}}{W_{2N}} \right), \quad (3)$$

where  $q_- = q_0 - |\mathbf{q}|$  and  $W_{2N}^2 = (q + 2m_N)^2 = -Q^2 + 4q_0m_N + 4m_N^2$ , with  $m_N$  the nucleon mass,  $q_0$  and  $\mathbf{q}$  representing energy and momentum transfer and  $Q^2 = \mathbf{q}^2 - q_0^2$ . This equation explicitly takes into account the recoil energy and momentum carried by the spectator nucleon in the 2N-SRC and ensures that solutions for  $\alpha_{2N}$  exist only for  $x \leq 2$ , where  $x = \frac{Q^2}{2m_N q_0}$  is the Bjorken variable. Additionally, in the limit of large  $Q^2$ ,  $\alpha_{2N} \approx x$ , and the variable  $x$  can replace  $\alpha_{2N}$  for identification of 2N SRCs in the large  $Q^2$  limit.

One of the important advantages of the LF treatment is that the cross section of inclusive scattering can be factorized into the electron-bound nucleon scattering cross section,  $\sigma_{eN}$  and light cone density matrix,  $\rho_A(\alpha_{2N})$ , in the following form[17, 38]:

$$\sigma_{eA} \approx \sum_N \sigma_{eN} \rho_A(\alpha_{2N}). \quad (4)$$

Note that within a non-relativistic framework no such simple factorization exists and the inclusive cross section is expressed through an integral over  $p_m^\perp$  and  $E_m$  of the convolution of  $\sigma_{eN}$  and the nuclear spectral function,  $S_A(p_m, E_m)$ , where  $p_m$  and  $E_m$  are missing momentum and energy in the reaction (see e.g. Ref. [38, 39]). The theoretical justification for the factorization in Eq. (4) in the high  $Q^2$  limit, is based on the validity of the closure approximation over the “plus”-component,  $p_+$ , of the 4-momentum of the bound nucleon in LF formalism (see e.g. Ref. [38]). The  $p_+$ -component in the LF formalism is analogous to the missing energy  $E_m$  and in the calculation of  $\sigma_{eN}$  is estimated at the average point,

corresponding to the 2N-SRC at rest,  $p_+ \approx 2m_N - \frac{m_N}{2-\alpha_{2N}}$ . Based on Eqs. (4) and (2) we predicted[1] that due to the dominance of 2N-SRC dynamics, the per-nucleon ratios of inclusive cross sections of nuclei and the deuteron:

$$a_2(A, Z) = \frac{2\sigma_{eA}(\alpha_{2N}, Q^2)}{A\sigma_{ed}(\alpha_{2N}, Q^2)}, \quad (5)$$

should scale with  $\alpha_{2N}$  for  $1.3 < \alpha_{2N} < 2$  and  $Q^2 > 1.5 \text{ GeV}^2$ , with the parameter  $a_2(A, Z)$  representing the probability of finding a 2N-SRC in nucleus,  $A$  relative to the deuteron. Here, the lower limit of  $\alpha_{2N}$  corresponds to the scattering off a bound nucleon with average momentum of  $p \gtrsim 0.3 \text{ GeV}/c$ .

The analysis of the available data[1] at that time from large  $Q^2$  inclusive experiments at SLAC was in agreement with the prediction of the scaling in Eq.(5). Subsequent dedicated experiments[2, 3, 6] at JLab confirmed this prediction and obtained similar estimates for the scaling parameter  $a_2(A, Z)$  for the wide range of atomic nuclei,  $A$  (see e.g. Fig.10 and the related discussion in Sec.VI.).

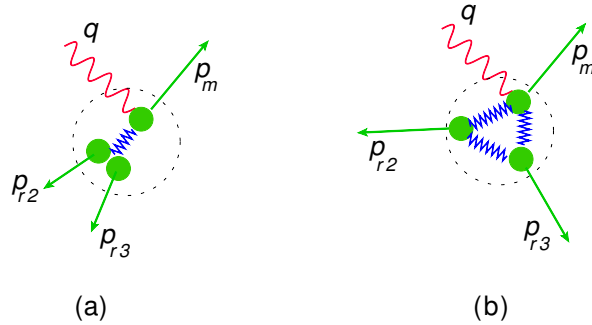


FIG. 1: Types of three nucleon SRCs. (a) In type 3N-I SRC the fast probed nucleon is balanced by two recoil nucleons with momenta  $\sim p_m/2$ . (b) In type 3N-II SRC all tree nucleons have equal momenta with relative angles  $\sim 120^\circ$ .

## B. 3N SRCs

For 2N-SRCs we considered the only possible configuration in which two fast nucleons are correlated back-to-back with a small center of mass momentum. For 3N-SRCs, however there are more configurations in which three fast nucleons can be associated with a small center of mass momentum. Two extreme cases of possible 3N-SRC configurations are presented in

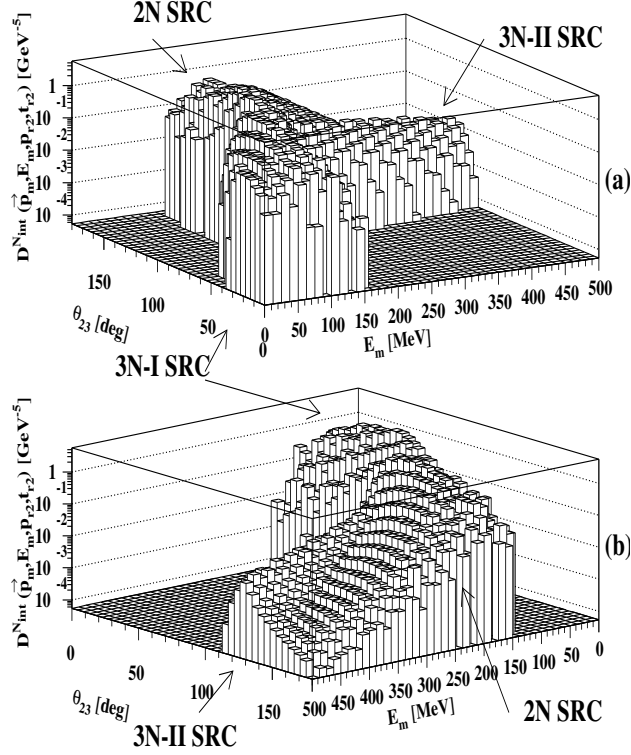


FIG. 2: Decay function for  ${}^3\text{He}$  nucleus calculated with the condition  $p_m \geq 700$  MeV/c, and  $p_{r2}, p_{r3} \geq k_F$ . The  $\theta_{23}$  is the relative angle between two recoil nucleons and  $E_m$  is the missing energy. Two panels show different point of views of the same figure. The figure is adapted from Ref.[19].

Fig. 1. The first, Fig.1(a), referred as type 3N-I SRC, corresponds to the situation in which the probed fast nucleon is balanced by two fast spectator nucleons  $p_{r2}, p_{r3} \sim p_m/2$  with a small relative angle between them, thus small invariant mass,  $m_S \sim 2m_N$ . The second case, Fig.1(b) corresponds to the symmetric situation in which all three nucleons have comparable momenta with relative angles  $\theta_{23} \sim 120^\circ$ .

To determine which of these 3N SRC configurations will dominate in inclusive  $A(e, e')X$  scattering it is instructive to consider the decay function for a three-body nucleus at large values of missing and recoil momenta, noticing that the integrated decay function enters in the cross section for inclusive scattering. The decay function has been calculated in Ref.[19, 40] for  ${}^3\text{He}$  using a realistic wave function based on the solution of Faddeev equations[41] and one of the results relevant for 3N-SRCs is presented in Fig. 2. In the figure a correlation between the relative angle of two recoil nucleons,  $\theta_{23}$  and missing energy  $E_m$  is presented



for  $p_m \geq 700$  MeV/c and  $p_{r2}, p_{r3} > k_F$ . As the figure shows the type 3N-I SRC provides the dominant contribution to the decay function at small missing energies,  $E_m \sim \frac{p^2}{4m_N}$ , with the relative angle between spectator nucleons  $\theta_{23} \leq 50^\circ$  (see Fig.2(a)). A transition to the type 3N-II SRC is observed with an increase of missing energy  $E_m \geq 200$  MeV, in which case  $\theta_{23} \sim 120^\circ$ . The analysis of type 3N-II SRCs[19] demonstrate that the irreducible three-nucleon forces have substantial contribution in this region due to large missing energies which increases the possibility of an inelastic  $N \rightarrow \Delta$  transition at the NN vertices of the correlation.

Since the integrated decay function, which enters in the inclusive cross section, is dominated by smaller values of  $E_m$ , one expects, based on the above discussion, that the type 3N-I SRC represents the main configuration contributing to the inclusive cross section. Based on this, it is possible to identify the kinematics at which 3N-SRCs can be isolated in inclusive scattering. Introducing mass  $m_S$  and momentum  $p_S$  for the two nucleon recoil system of type 3N-I SRC (Fig.1(a)) we consider energy-momentum conservation in quasielastic scattering from a 3N-SRC which takes the form:

$$q + 3m_N = p_f + p_S. \quad (6)$$

Here  $q$  is the four momentum transfer and  $p_f$  is the final 4-momentum of the struck nucleon in the 3N SRC. Using boost invariance of the light-cone momentum fractions, for the spectator system in the  $\gamma - 3N$  center of mass frame, we define the ratio:

$$\frac{p_s^-}{p_{\gamma 3N}^-} = \frac{E_S^{cm} + p_{S,z}^{cm}}{E_S^{cm} + E_f^{cm}} \approx \frac{E_S^{cm} + p_S^{cm}}{W_{3N}}, \quad (7)$$

where  $W_{3N}$  is the invariant mass produced from the interaction with the 3N system:

$$W_{3N}^2 = (q + 3m_N)^2 = Q^2 \frac{3-x}{x} + 9m_N^2. \quad (8)$$

In the RHS of Eq.(7) we neglected the transverse momentum of the spectator NN system as it is integrated over in inclusive reactions. This is justified since the inclusive cross section is dominated by kinematics in which  $p_{S,\perp} \ll p_{S,z}$ . Furthermore  $E_S^{cm}$  and  $p_S^{cm}$  can be calculated through  $W_{3N}$  using the relation:

$$E_S^{cm} = \frac{W_{3N}^2 - m_N^2 + m_S^2}{2W_{3N}} \quad \text{and} \quad p_S^{cm} = \sqrt{E_S^{cm,2} - m_S^2}, \quad (9)$$

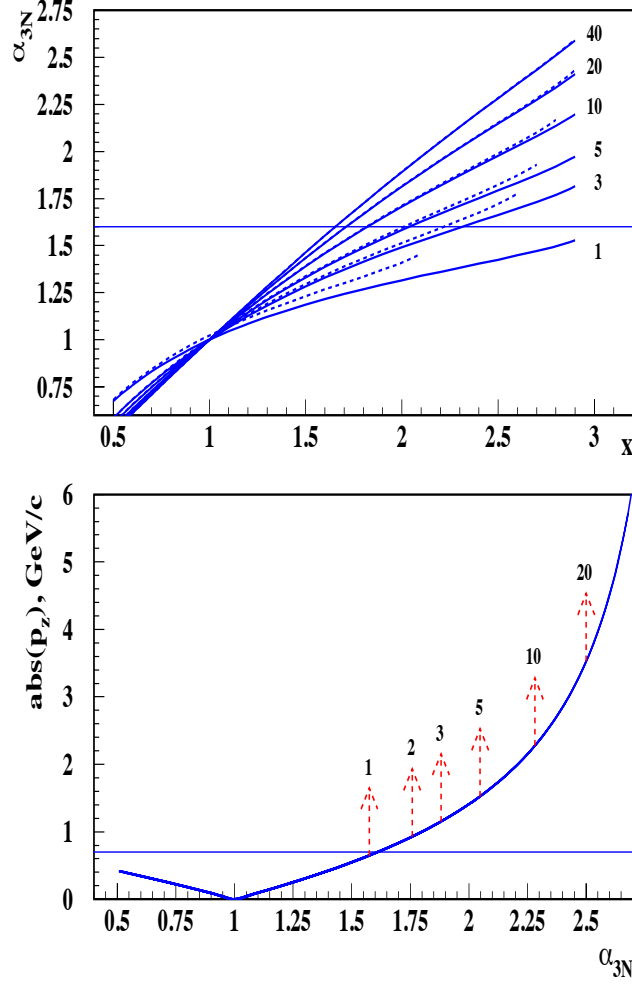


FIG. 3: Kinematics of 3N SRCs. (upper panel) Relation between  $\alpha_{3N}$  and  $x$  for  $m_S$  calculated according to Eq.(10) with  $k = 0$  (dotted line) and  $k = 250$  MeV/c.(dashed line). The curves are labeled by their respective  $Q^2$  values. (lower panel) The dependence of  $|p_z|$  on  $\alpha_{3N}$ . Arrows indicate the maximum possible  $\alpha_{3N}$ 's that can be reached at given values of  $Q^2$ .

where  $m_S$  is defined as:

$$m_S^2 = 4 \frac{m_N^2 + k_\perp^2}{\beta(2 - \beta)}, \quad (10)$$

with  $k_\perp$  representing the transverse component of the relative momentum of the spectator nucleons with respect to  $\vec{p}_S$ .  $\beta$  is the light-cone momentum fraction of  $p_S$  carried by one of the spectator nucleons and is normalized to be  $0 \leq \beta \leq 2$ .

Eq.(7) can be used to estimate the light-cone momentum fraction of the nucleon in a

3N-SRC by observing that  $\alpha_{3N} = 3 - \alpha_S$ , where  $\alpha_S = 3 \frac{p_S^-}{p_{3N}^-}$ :

$$\alpha_{3N} = 3 - 3 \frac{p_S^-}{p_{3N}^-} = 3 - 3 \frac{p_S^-}{p_{\gamma 3N}^-} \frac{p_{\gamma 3N}^-}{p_{3N}^-}, \quad (11)$$

where we again exploit the boost invariance of the ratio of  $\frac{p_{\gamma 3N}^-}{p_{3N}^-} = \frac{q_- + 3m_N}{3m_N}$  along  $\mathbf{q}$ . This results in the following expression for the light-cone momentum fraction of the fastest nucleon belonging to 3N-SRCs:

$$\alpha_{3N} = 3 - \frac{q_- + 3m_N}{2m_N} \left[ 1 + \frac{m_S^2 - m_N^2}{W_{3N}^2} + \sqrt{\left(1 - \frac{(m_S + m_n)^2}{W_{3N}^2}\right) \left(1 - \frac{(m_S - m_n)^2}{W_{3N}^2}\right)} \right]. \quad (12)$$

Using this equation we can identify the kinematical conditions for  $x$  and  $Q^2$  for which the inclusive cross section is dominated by scattering from a nucleon in a 3N SRC. For this, we first need to determine the threshold value for  $\alpha_{3N}^0$  above which one expects the onset of 3N-SRC dynamics. We also need an estimate of  $m_S$  through Eq.(10). We note that for inclusive  $A(e, e')X$  scattering the cross section is defined by the nuclear light-cone density matrix in which one integrates over the range of the two-nucleon spectator system masses  $m_S \geq 2m_N$ . This integral however is dominated by  $\beta \sim 1$  with the recoil nucleon's momentum,  $k$  relative to  $p_S$  not exceeding the nuclear Fermi momentum,  $k_F \approx 250$  MeV/c (see e.g. Ref.[19]). Hence, for numerical estimates we consider two values: for  $k = 0$  and  $k = 250$  MeV/c.

With these considerations and Eq.(12) we identify the most favorable domain in  $x$  and  $Q^2$  to search for 3N-SRCs in inclusive  $A(e, e')X$  reactions. In Fig.3(upper panel) we present the  $\alpha_{3N} - x$  relation for different values of  $Q^2$ . The solid and dashed curves correspond to the spectator mass,  $m_S$  calculated according to Eq.(10) with  $k = 0$  and  $k = 250$  MeV/c. Figure 3 shows that at  $Q^2 \approx 3$  GeV<sup>2</sup> there exists a finite kinematic domain with  $\alpha_{3N} \geq 1.6$  where one expects the onset of the 3N-SRC dominance. In addition, starting with  $Q^2 \geq 5$  GeV<sup>2</sup> the onset of 3N-SRCs is practically insensitive to the recoil mass of the spectator system,  $m_S$ . As it follows from the figure, for  $Q^2 \gtrsim 3$  and 5 GeV<sup>2</sup> the magnitudes of  $x \gtrsim 2.2$  and  $x \gtrsim 2$  respectively are necessary to probe  $\alpha_{3N} > 1.6$ . Furthermore, using the relation,

$$\alpha_S = 3 - \alpha_{3N} \approx \frac{\sqrt{m_S^2 + p_z^2} + p_z}{m_N}, \quad (13)$$

we can calculate the longitudinal component of the initial momentum of the struck nucleon,  $p_z$ , which is the minimal possible momentum of the nucleon in 3N-SRC. According to the 3N-

SRC scenario this momentum,  $p_z$ , is equal and opposite to the center of mass momentum of the recoil two-nucleon system. It is worth mentioning that this momentum does not appear directly in the argument of the light-cone nuclear wave function but enters through the nonlinear relation of Eq.(13). Nonetheless it gives an estimate of the bound nucleon momenta to be reached in a fixed target experiment aimed at probing 3N SRCs. Fig.3(b) shows the dependence of  $|p_z|$  on  $\alpha_{3N}$  with the arrows indicating the maximum possible  $\alpha_{3N}$ 's that can be probed at given values of  $Q^2$ . One observes from the plot that the characteristic momenta of the struck nucleon in the 3N SRCs for  $\alpha_{3N} \geq 1.6$  is  $p_z \gtrsim 700$  MeV/c.

### III. DYNAMICS OF THE 3N SRCs

In light of the recent observation of strong dominance of the  $pn$  component in 2N-SRCs[5, 18, 22] within the momentum range of 250 – 650 MeV/c and the assertion (discussed above) that type 3N-I SRCs dominate in inclusive scattering at  $\alpha > 1.6$  and  $|p_z| \gtrsim 0.7$  GeV/c one expects that the main mechanism for generation of 3N-SRCs is due to successive  $pn$  short range interactions[17, 28, 42] with the mass of the spectator 2N system tending to be small,  $m_S \sim 2m_N$ . Due to  $pn$  dominance 3N-SRCs should have predominantly  $ppn$  or  $nnp$  composition with  $ppp$  and  $nnn$  configurations being strongly suppressed. The diagram representing the light-cone density matrix of 3N SRCs is given in Fig.4 where three-nucleon lines are  $ppn$  or  $nnp$  configurations.

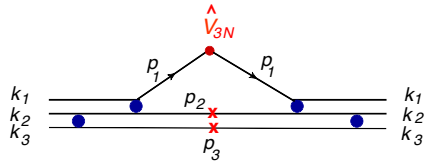


FIG. 4: The 3N SRCs due to successive  $pn$  short range correlations. Here  $k_i$  and  $p_i$  are shorthand notations for the light-cone momenta  $(\beta_i, k_{i,\perp})$  and  $(\alpha_i, p_{i,\perp})$ . The figure is adapted from Ref.[28].

Calculation of the 3N-SRC contribution to the nuclear density matrix according to dia-

grams similar to Fig. 4 yields[28]:

$$\begin{aligned} \rho_{3N}(\alpha_1) = & \int \frac{1}{4} \left[ \frac{3 - \alpha_3}{(2 - \alpha_3)^3} \rho_{pn}(\alpha_3, p_{3\perp}) \rho_{pn} \left( \frac{2\alpha_2}{3 - \alpha_3}, p_{2\perp} + \frac{\alpha_1}{3 - \alpha_3} p_{3\perp} \right) + \right. \\ & \left. \frac{3 - \alpha_2}{(2 - \alpha_2)^3} \rho_{pn}(\alpha_2, p_{2\perp}) \rho_{pn} \left( \frac{2\alpha_3}{3 - \alpha_2}, p_{3\perp} + \frac{\alpha_1}{3 - \alpha_2} p_{2\perp} \right) \right] \delta \left( \sum_{i=1}^3 \alpha_i - 3 \right) \\ & d\alpha_2 d^2 p_{2\perp} d\alpha_3 d^2 p_{3\perp}, \end{aligned} \quad (14)$$

where  $(\alpha_i, p_{i\perp})$ ,  $(i = 1, 2, 3)$  are light-cone momentum fractions and transverse momenta of nucleons and  $\rho_{pn}(\alpha, p_{\perp})$  is the density matrix of  $pn$ -SRC. The prevalence of  $\rho_{3N}$  in a nuclear density function,  $\rho_A$ , in 3N-SRC region suggests several characteristics that can be experimentally verified. The one follows from Eq.(5), according to which  $\rho_{pn} \sim a_2(A, z)\rho_d$  and therefore the per nucleon probability of finding a nucleon in a 3N-SRC,  $a_{3N}$ , should be proportional to the square of the probabilities of 2N SRCs,  $a_{2N}$ , (actual relation will be given in Sec.V):

$$a_{3N}(A, Z) \sim a_{2N}(A, Z)^2. \quad (15)$$

Another feature follows from the expectation that the mass of the recoil 2N system,  $m_S$ , in 3N-SRC is small, which results in a small relative momentum in the recoiling NN system,  $k = \frac{\sqrt{m_S^2 - 4m_N^2}}{2}$ . The condition  $k \ll m_N$  and the fact that iso-triplet two-nucleon states with low relative momentum are strongly suppressed compared to the iso-singlet states[19] produces a strong sensitivity of the 3N-SRCs on the isospin structure of NN recoil system. Namely, the dominant 3N-SRC configurations are those which have a recoil two nucleons in the iso-singlet state. This situation is illustrated in Fig. 5 where the high momentum distribution of protons and neutrons in  $^3\text{He}$ , calculated in Variational Monte Carlo (VMC) approach[43], is compared with the calculation based on the 2N and 3N SRC model of Ref. [28], the latter being based on Eq. (14). Fig. 5 shows the 2N-SRC model completely describes the neutron momentum distribution up to 1 GeV/c, while one needs 3N-SRC contributions to describe the proton momentum distribution above 700 MeV/c. This result is in agreement with the dominance of iso-singlet recoil NN systems in the generation of 3N-SRCs. For the case of the neutron, the recoil system is a  $pp$  pair, which is strongly suppressed as compared with that of the proton, in which case the recoil system is in the isosinglet  $pn$  state where no suppression exists. Notice, that even if the 3N-SRCs contribute to the proton momentum distribution in  $^3\text{He}$  it is still a correction to the main 2N-SRC part of the momentum distribution as discussed in Sec. I.

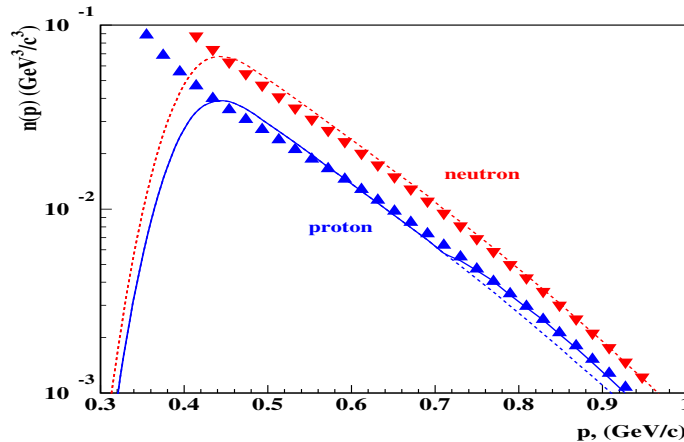


FIG. 5: The momentum distribution of the proton and neutron in  $^3\text{He}$ . The triangle symbols are from the VMC calculation of Ref.[43]. The dashed lines are contributions from 2N SRCs only, solid lines correspond to the combined contributions from 2N and 3N SRCs[28]. In the case of the neutron distribution no 3N SRCs are included.

It is worth mentioning that type 3N-II SRCs can be described through diagrams similar to Fig. 4 in which case the intermediate state between two successive NN interactions has a large invariant mass. Here another source of 3N-SRCs could be the configuration containing a  $\Delta$ -resonance in the intermediate state, which will represent the contribution from “genuine” three-nucleon forces irreducible to NN interactions. As it was discussed in Sec.II one expects that type 3N-I SRCs should be the dominant source of 3N correlations in inclusive reactions. Probing type 3N-II SRCs will require semi-inclusive processes in which the recoiling two-nucleon system has a large invariant mass.

#### IV. FINAL STATE INTERACTIONS

Final state interactions (FSI) can both distort and mimic 3N SRCs. Detailed quantitative studies of the FSI effects are clearly necessary. Below we provide several qualitative considerations based on the high energy nature of electro-production reactions which are used to probe 3N-SRCs.

The source of the distortion is mainly due to the multiple rescattering of nucleons from 3N SRCs with the nucleons belonging to the “uncorrelated” spectator (A-3) system. An example is presented in Fig.6(a) in which a nucleon knocked-out from a 3N-SRC rescatters off

the uncorrelated nucleons in the (A-3) residual nucleus. Other examples are the rescattering of spectator nucleons in the 3N-SRC with the uncorrelated nucleons from (A-3) system. For such rescatterings, because of inclusive nature of the process, one integrates over the range of excitation energies of the (A-3) system. As a result the closure approximation can be applied (see discussion in Sec.II) which cancels the effects of long-range FSIs. The empirical evidence for such cancellation follows from the experimental observation of the 2N-SRC scaling in the  $1 < x < 2$  domain[1–3, 6] (also Sec.II) in which case the closure condition is satisfied for the FSI with residual (A-2) nucleus.

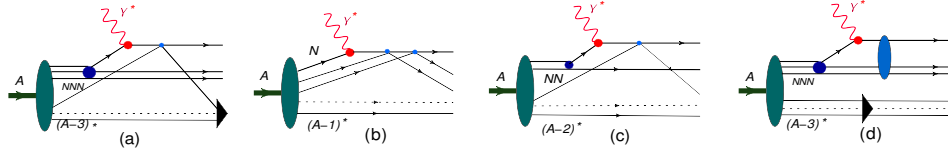


FIG. 6: Possible FSI diagrams contributing in 3N SRC kinematics. Detailed description given in the text.

FSIs that can in principle mimic 3N-SRCs are diagrammatically presented in Fig.6 (b) and (c). In the case of (b) an uncorrelated nucleon in the mean field with initial LC momentum fraction,  $\alpha_N \approx 1$ , is struck and two successive rescatterings may increase the momentum fraction to  $\alpha_N \gtrsim 1.6$ , making it appear as a nucleon from 3N-SRC. In the case of (c) a nucleon knocked out of a 2N-SRC where the characteristic momentum fraction is  $1.3 \leq \alpha_N \leq 1.5$  and FSI could shift it to the  $\alpha_N \gtrsim 1.6$  region. An important feature that suppresses the migration of  $\alpha_N$  into the 3N-SRC region is the approximate conservation of the LC momentum fraction in high energy (eikonal) regime of small angle rescattering[38, 39]. In this case the non-conservation of  $\alpha_N$  is estimated as[38, 39]:

$$\delta\alpha \approx \frac{x^2}{Q^2} \frac{2m_N E_R}{\left(1 + \frac{4m_N^2 x^2}{Q^2}\right)}, \quad (16)$$

where  $E_R = \sqrt{m_S^2 + p^2} - m_S$  and  $p \sim 0.7 - 1$  GeV/c is the characteristic momentum of the nucleon in a 3N-SRC.

In Fig. 7 we present the  $Q^2$  dependence of the non-conservation of  $\alpha_N$  for  $2 \leq x \leq 2.9$ . The estimates are made for  $p = 1$  GeV/c and  $m_S = 2m_N$ . It follows from the figure that for  $Q^2 > 3$  GeV<sup>2</sup> that FSI may alter  $\alpha_N$  by no more than 0.14 which is too small to shift the mean field nucleon,  $\alpha_N \approx 1$ , to the 3N SRC domain. However one may expect possible FSI

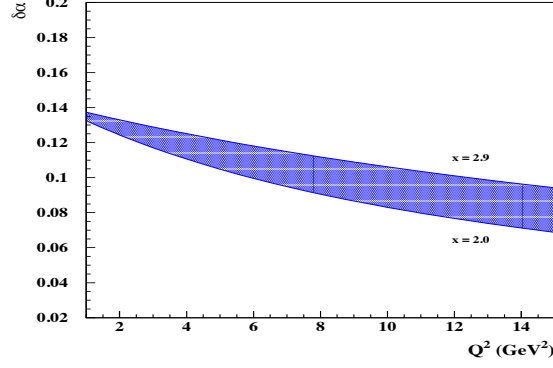


FIG. 7: Non-conservation of  $\alpha_N$  as a function of  $Q^2$  according to Eq.(16) for  $p = 1$  GeV/c and  $2 \leq x \leq 2.9$ .

contribution from the 2N-SRC domain,  $1.3 \leq \alpha_{2N} \leq 1.5$ , influencing the onset of 3N SRCs at  $\alpha_{3N} \sim 1.6$ .

Finally, the other FSI effects follow from the rescattering within a 3N-SRC as shown in Fig.6 (d). In this case one expects a modification of the  $p_\perp$  distribution in the 3N SRCs. However the important feature of high energy small angle re-scattering, discussed above, is that while FSI redistributes transverse momenta, it leaves the  $\alpha_N$  distribution almost intact (see also Ref.[44]). As a result the measured inclusive cross section in the 3N-SRC domain can be presented in the factorized form similar to the 2N-SRC case (Eq.(4)):

$$\sigma_{eA} \approx \sum_N \sigma_{eN} \rho_A^N(\alpha_{3N}), \quad (17)$$

where

$$\rho_A^N(\alpha_{3N}) = \int \rho_A^N(\alpha_{3N}, p_\perp) d^2 p_\perp, \quad (18)$$

is weakly modified due to FSI, even if the  $p_\perp$  distribution of the unintegrated nuclear density matrix,  $\rho_A^N(\alpha, p_\perp)$  is distorted by the FSI [44].

In the discussion above we focused only on the part of the FSI which corresponds to the pole contribution from the struck nucleon propagator, representing the on-shell propagation of the fast nucleon in the intermediate state. Another contribution to FSI comes from the non-pole term of the FSI amplitude in which case the struck nucleon is highly virtual. There are two main sources of the suppression of the off-shell FSI contribution. First, the off-shell FSI contribution is proportional to the square of the real part of the  $NN$  scattering amplitude which is, smaller by an order of magnitude, than the imaginary part (see e.g.



[45, 46]). Second, due to the large virtuality of the fast nucleon the off-shell  $NN$  rescattering amplitude is strongly suppressed[47]. There is also an empirical evidence from the studies of 2N-SRCs that off-shell rescattering amplitudes are negligible[1].

## V. 3N SRC OBSERVABLES

The experimental observation of 3N-SRCs is challenging for many reasons. As Fig. 5 shows, that simply extracting the momentum distribution at  $\gtrsim 700$  MeV/c will not allow the isolation of 3N-SRCs due to substantial 2N-SRC contribution. Furthermore, the 3N-SRC contribution to the momentum distribution decreases faster with an increase of momentum than the 2N-SRC contribution. Overall, the bound nucleon momentum is not a good parameter with which to explore 3N-SRCs. The more natural parameter, as it was discussed earlier, is the light-cone momentum fraction  $\alpha_N$  for which according to Eq.(2) the condition  $\alpha_N \gtrsim 2$  will completely isolate 3N-SRCs with the transition region expected to start at  $\alpha_N \gtrsim 1.6$ .

Moreover, according to Eq.(17) the cross section of inclusive reaction factorizes in the form of the product of electron - nucleon cross section and the  $p_\perp$  integrated light-cone density matrix,  $\rho_A(\alpha_{3N})$ . Hence, the appropriate observable for 3N SRCs is the ratio of inclusive  $A(e, e')X$  cross sections for nuclei  $A_2$  and  $A_1$  in the region of  $\alpha_{3N} \geq \alpha_{3N}^0$  and  $Q^2 > 3 \text{ GeV}^2$ :

$$R_{A_1}(A_2) = \frac{A_1 \sigma_{A_2}(x, Q^2)}{A_2 \sigma_{A_1}(x, Q^2)} \Big|_{\alpha_{3N} > \alpha_{3N}^0} . \quad (19)$$

In this case  $\alpha_{3N}^0$  (expected to be  $\sim 1.6$ ) should be defined from the observation of the onset of a plateau in the  $\alpha_{3N}$  dependence of the ratio  $R_{A_1}(A_2)$ . Note that in Eq.(19) the off-shell effects in electron-bound nucleon scattering are mostly cancelled in the ratio.

The observation of a plateau assumes also that  $\alpha_{3N}$  is insensitive to the recoil mass of the spectator 2N system,  $m_S$ , over which the cross section of the inclusive scattering is integrated. This imposes an additional condition for the observation of scaling. This insensitivity is shown in Fig. 8 and is largely achieved at  $Q^2 \geq 5 \text{ GeV}^2$ . However the expectation that the integral over the recoil mass will saturate in the range of  $2m_N \leq m_S \leq 2 \text{ GeV}$ [19] indicates a possibility of an early onset of the plateau already at  $Q^2 = 3 \text{ GeV}^2$ .

In the region of  $\alpha_{3N} < \alpha_{3N}^0$  at modest  $Q^2$  ( $\leq 3 \text{ GeV}^2$ ) one expects an existence of pre-asymptotic domain where the ratios (19) are not constant as a function of  $\alpha_{3N}$  but are

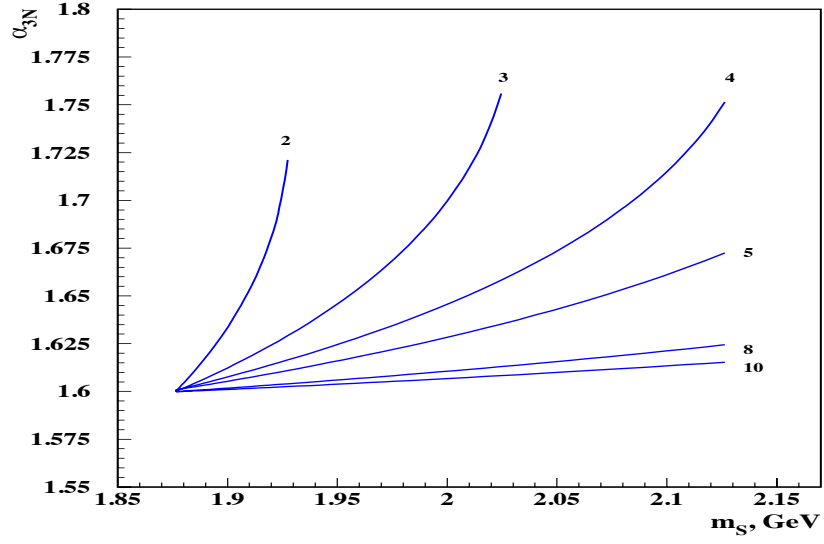


FIG. 8: Dependence of  $\alpha_{3N}$  on the recoil mass,  $m_s$  of the spectator system in 3N SRC for different values of  $Q^2$ , calculated according to Eq.(12).

largely  $Q^2$  independent for fixed  $\alpha_{3N}$ . This is mainly due to the factorization of the inclusive cross section in the form of Eq. (17). Such a behavior would be analogous to the pattern observed for  $\alpha_{2N}$  dependence of the ratio (5) at  $\alpha_{2N} < 1.3$ [1]. This analogy is reinforced in Fig. 9 where one observes that  $\alpha_{2N}$  and  $\alpha_{3N}$  are nearly identical for  $x < 1.6$ .

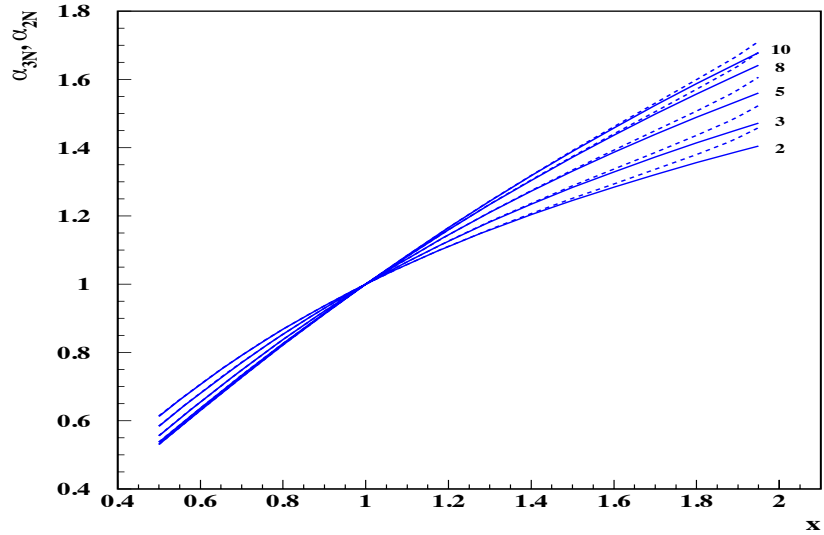


FIG. 9: The  $x$  dependence of  $\alpha_{3N}$  (solid lines) and  $\alpha_{2N}$  (dashed lines) at different  $Q^2$ .

To connect the ratio  $R_{A_1}(A_2)$ , defined in Eq.(19), with theoretical calculations of nuclear density function we introduce parameter  $a_3(A, Z)$  characterizing the probability of 3N SRCs for nearly symmetric nuclei as follows:

$$a_3(A, Z) = \frac{3}{A} \frac{\sigma_{eA}}{(\sigma_{e^3He} + \sigma_{e^3H})/2}. \quad (20)$$

This parameter can be related to the ratio  $R_3(A, Z)$  which is defined in Eq.(19) for  $A_2 = A$  and  $A_1 = {}^3\text{He}$ . The ratio  $R_3(A, Z)$  is the most accessible experimental quantity.

Based on the factorization of Eq.(17), for  $R_3(A, Z)$  and  $a_3(A, Z)$  one obtains:

$$R_3(A, Z) = a_3(A, Z) \frac{(\sigma_{ep} + \sigma_{en})/2}{(2\sigma_{ep} + \sigma_{en})/3}. \quad (21)$$

Thus, a measurement of the ratio  $R_3(A, Z)$  will allow an extraction of the parameter  $a_3(A, Z)$  which can be used for verification of the theoretical models of 3N SRCs.

Based on the above definitions we can also formulate an experimental observable which will allow us to verify the prediction of Eq.(15). For this, we notice that for type 3N-I SRC (Fig.1(a)) the calculation of nuclear density function[28] (Eq.(14)) yields:

$$a_3(A, Z) = \frac{a_2(A)^2}{a_2^p({}^3\text{He})a_2^n({}^3\text{He})}, \quad (22)$$

where  $a_2^p$  and  $a_2^n$  are per-nucleon probabilities of finding proton or neutron in 2N SRC. One can relate these parameters to the parameter  $a_2(A, Z)$  of Eq.(5) using the estimate of high momentum part of the proton and neutron distributions in nuclei within the  $pn$ -dominance model in the form[21]:

$$n_2^{p/n}(p) = \frac{a_2(A)}{2X^{p/n}} n_d(p), \quad (23)$$

where  $X^{p/n} = \frac{Z(N)}{A}$  is the relative fraction of the protons or neutrons and  $n_d(p)$  is the high momentum distribution of the deuteron. According to Eq.(23) one estimates:

$$a_2^n({}^3\text{He}) = \frac{a_2({}^3\text{He})}{2/3} \quad \text{and} \quad a_2^p({}^3\text{He}) = \frac{a_2({}^3\text{He})}{4/3}, \quad (24)$$

where  $a_2({}^3\text{He})$  is defined according to Eq.(5).

Using above estimates together with Eq.(21) and Eq.(22) one obtains:

$$\begin{aligned} R_3(A, Z) &= \frac{9}{8} \frac{(\sigma_{ep} + \sigma_{en})/2}{(2\sigma_{ep} + \sigma_{en})/3} \left( \frac{a_2(A, Z)}{a_2({}^3\text{He})} \right)^2 = \\ &= \frac{9}{8} \frac{(\sigma_{ep} + \sigma_{en})/2}{(2\sigma_{ep} + \sigma_{en})/3} R_2^2(A, Z), \end{aligned} \quad (25)$$

where in the last part of the equation we used the fact that the variables  $\alpha_{2N}$  and  $\alpha_{3N}$  have nearly same magnitudes in the 2N-SRC region (see in Fig.(9)) to relate the ratios of  $a_2$  parameters to experimentally measured ratio:

$$R_2(A, Z) = \frac{3}{A} \frac{\sigma_{eA}}{\sigma_{e^3H}} \Big|_{1.3 < \alpha_{3N} < 1.5} = \frac{a_2(A)}{a_2(^3He)}. \quad (26)$$

In the following section we will analyze experimental data at  $Q^2 \sim 3 \text{ GeV}^2$  for which  $\sigma_{ep} \approx 3\sigma_{en}$ . This, according to Eq.(25) yields:

$$R_3(A, Z) \approx \frac{54}{56} R_2(A, Z)^2 \approx R_2(A, Z)^2. \quad (27)$$

Equations (25) and (27) present a remarkable prediction, that the ratios of inclusive nuclear cross sections ( $R_2$  and  $R_3$ ) measured at different domains of  $\alpha_{3N}$  will be related by simple quadratic relation if the scattering in the  $\alpha_{3N} > \alpha_{3N}^0$  region probes type 3N-I SRCs.

## VI. EXPERIMENTAL EVIDENCE FOR 3N SRCS

Conclusive evidence for two-nucleon SRCs first appeared in 1993[1] from the analysis of data from different experiments at SLAC. The SLAC data sets for light nuclei did not share common kinematics with the data for heavy nuclei[48] and it was necessary, after re-binning into common x-bins, to interpolate the deuteron data across  $Q^2$  to form the ratios of inclusive cross sections for nuclei  $A$  and the deuteron ( $\frac{2\sigma_A}{A\sigma_D}$ ). The plateau for the available nuclei in these ratios had a weak  $A$  dependence for  $A \geq 12$ . The ratios were smaller for  $^3\text{He}$  and  $^4\text{He}$  (with large error bars). The  $\frac{3\sigma_A}{A\sigma_{^3He}}$  ratios from Hall B at JLab showed similar plateaus[2, 3]. These measurements provided persuasive evidence for the presence of 2N SRCs yet were limited in their precision and/or the desired expansive range in  $x$  and  $Q^2$ . E02-019[6, 36] produced high quality data in the 2N-SRC region - these are reproduced in Fig. 10.

The data available to study 3N-SRCs are sorely limited.  $^3\text{He}$  data (SLAC[15], Hall B [2, 3], Hall C [6] and Hall A [33] at Jefferson Lab) provided good agreement for the height of the 2N-SRC plateau for  $x < 1.5 < 2.0$  yet there are significant disagreements in the  $x > 2$  region. These arise from the fact that the SLAC and data from Jefferson Lab's Hall A[33] are at the lower limit of the range of  $Q^2$  necessary to study 3N correlations and the same is true for a fraction of the data from CLAS[2, 3]. The reliability of the observed scaling in the  $x > 2$  region for CLAS data was questioned in Ref.[34] which observed that the modest

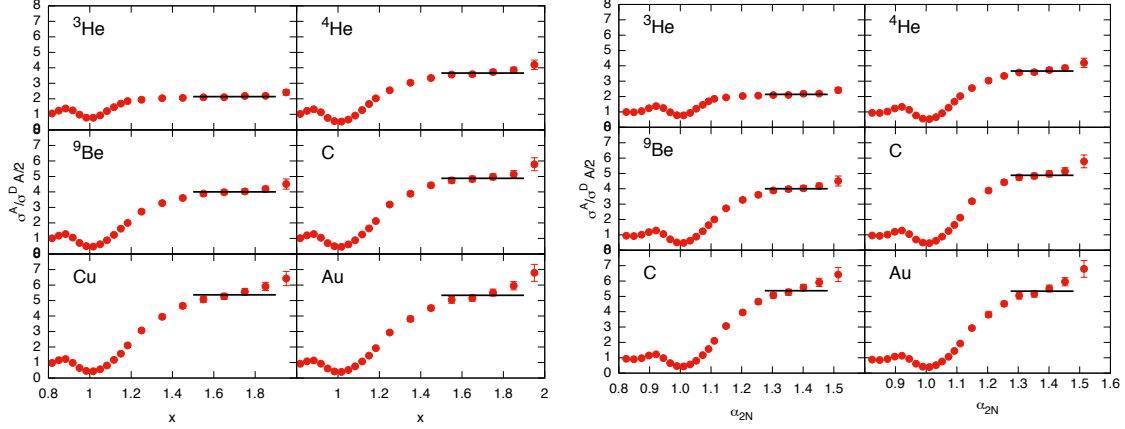


FIG. 10: Data from E02-019[6, 36] showing the ratios of  $\frac{2\sigma_A}{A\sigma_D}$  against  $x$  and  $\alpha_{2N}$  (right). The horizontal lines are the  $a_2$  plateau values taken from [6].

momentum resolution of the CLAS detector in Hall B allows, when the cross sections are falling steeply with  $x$ , bin migration, in which events in a reconstructed  $x$ -bin originated in a lower  $x$ -bin. To get a sense for paucity of the data, we show in Fig. 11 the kinematic extent of all published  $^3\text{He}$  data cited above as a scatter plot of  $Q^2$  and  $x$  (top) and  $Q^2$  and  $\alpha_{3N}$  (bottom). As it can be seen only a small fraction of the data satisfy the necessary condition of  $Q^2 \gtrsim 3 \text{ GeV}^2$  and  $\alpha_{3N} \gtrsim 1.6$  as indicated by the vertical line even though the large set of data to the right of the vertical line at  $x = 2$  in the top panel might suggest otherwise.

Experiment E02-109[49–52] was developed with the goal, in part, to provide precision ratios, in the 2N-SRC region, at large momentum transfer for a wide range of nuclei. The ratios,  $(\frac{2\sigma_A}{A\sigma_D})$ , at  $Q^2 \approx 2.75 \text{ GeV}^2$  (at  $x = 1$ ) indicated scaling patterns expected for 2N-SRC region[6]. The heights of the plateaus at  $x > 1.5$  scale approximately with  $A$ [6] (see Fig. 10) and have been related to the parameter  $a_2(A, Z)$  (Eq. 5) characterizing the probability of finding 2N-SRCs in nucleus  $A$  relative to the deuteron.

To check whether  $\alpha_{3N}$  description of the data results in the factorization implicit in Eq. (17), in Fig. 12 we compare the  $x$  and  $\alpha_{3N}$  dependences of  $\frac{3\sigma_A}{A\sigma_{^3\text{He}}}$  for all available  $Q^2$  from Refs. [6, 36] for  $A = 12$ . As the comparison shows the  $Q^2$  spread of the data is significantly reduced once the ratios are evaluated in terms of  $\alpha_{3N}$  which absorbs part of the  $Q^2$  dependence. The plateau in the region  $1.3 < \alpha_{3N} < 1.5$  manifests the dominance of 2N-SRCs corresponding, here, to internal nucleon momenta in the range of 300 – 600 MeV/c. The plateaus arising from 2N-SRCs in the ratios as a function of  $\alpha_{3N}$  (similar to  $\alpha_{2N}$ ) can

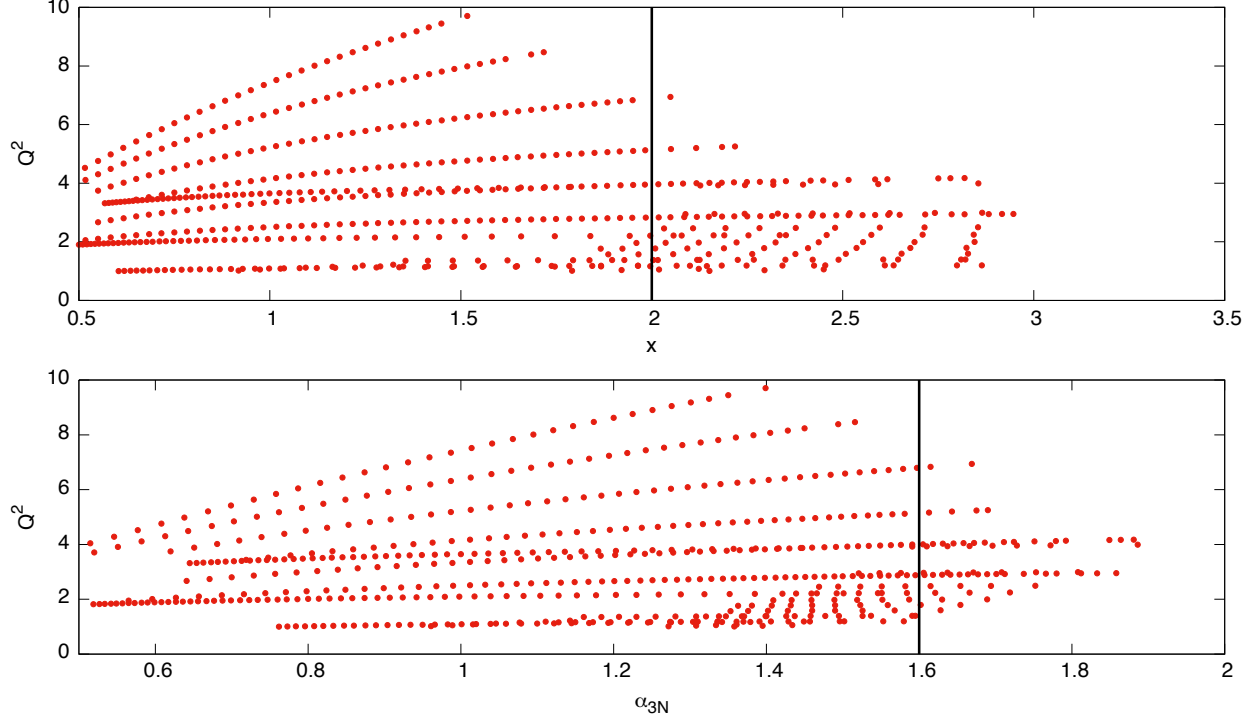


FIG. 11: Kinematic distribution of the world data set for  ${}^3\text{He}$  with  $Q^2 > 1$ :  $Q^2$  versus  $x$  (top) and  $Q^2$  versus  $\alpha_{3N}$  (bottom). Only data with  $\alpha_{3N} > 1.6$  is used when considering 3N-SRC as indicated by the black vertical line in the bottom panel. The kinematic points above do not necessarily imply corresponding data for other nuclei. It should be noted that at very large  $x$  and  $\alpha_{3N}$  the data have large relative errors.

be seen as following from the fact (see Fig. 9) that numerically  $\alpha_{2N}$  and  $\alpha_{3N}$  have small differences at  $Q^2 > 2 \text{ GeV}^2$  and  $x < 1.8$ . The observation of 2N-SRCs in terms of  $\alpha_{3N}$  is important for verifying the conjecture (Eq. 27)) that a plateau, if observed, in the 3N-SRC region should be proportional to  $(\frac{a_2(A)}{a_2({}^3\text{He})})^2$ .

As Fig.12 shows only measurement at  $18^\circ$ , (in which  $Q^2 \simeq 2.5 (\text{GeV}/c)^2$  at the quasielastic peak, growing to  $Q^2 \simeq 3 (\text{GeV}/c)^2$  at  $x = 2.9$ ) reaches to the region  $\alpha_{3N} \simeq 1.6$  where one expects the onset of 3N SRCs. It is intriguing that as the lower panel of the figure shows at  $\alpha_{3N} > 1.6$  the ratios indicate possible onset of the scaling. In the further discussions, except where explicitly indicated our analysis of [6] is limited to these data set.

Problems arose when constructing the  ${}^3\text{He}$  cross section between  $x = 2.68$  and  $x = 2.85$  ( $1.6 \leq \alpha_{3N} \leq 1.8$ ) due to difficulties with the subtraction of the walls of the Aluminum target cell containing the  ${}^3\text{He}$ . The limited vertex resolution of the spectrometer made it

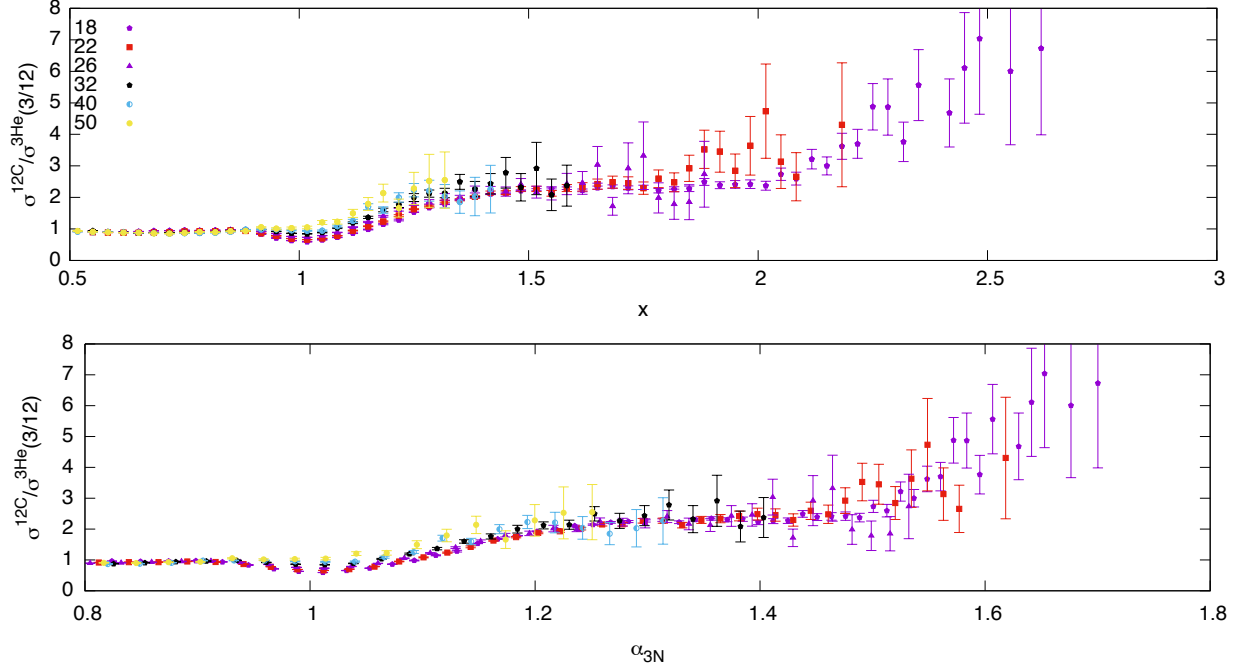


FIG. 12: The  $x$  and  $\alpha_{3N}$  dependences of the per-nucleon ratios of  $^{12}\text{C}/^3\text{He}$  for different angles with  $Q^2$  ranging from  $2.5 - 7.5 \text{ GeV}^2$  (at  $x = 1$ ) against  $x$  (top) and  $\alpha_{3N}$ . Only data with relative errors less than 0.5 are shown.

impossible to isolate electrons that scattered from the walls of the relatively small diameter (4 cm) target cell. This and the fact that  $\sigma^{\text{Al}} \gg \sigma^{\text{He}}$  at large  $x$  as  $\sigma^{\text{He}}$  must go to 0 at its kinematic limit,  $x = 3$ . resulted in a set of negative cross sections in three bins at large  $x$  interlaced with other bins in which cross sections were consistent with zero with large relative errors.

In contrast, the data in the region below  $x < 2.5$  are of excellent quality with small errors. As expected a  $y$ -scaling analysis[54, 55] of the E02-019 data found it to be in good agreement with the SLAC data[12, 15] from  $y = 0$  (top of the quasielastic peak) to  $y \simeq -1$  (GeV/c). In Fig. 13 we plot the scaling function  $F(y)$  against  $y$  with the inset showing (in a linear scale) the region  $-1.1 < y < -0.7$  and where the negative values of  $F(y)$  arise from the negative  $^3\text{He}$  cross sections mentioned above.

Despite the negative  $^3\text{He}$  cross sections the ratio,  $\frac{^4\text{He}}{^3\text{He}}$ , over the entire  $x$ -region from E02-019 were formed and published in Ref. [6] by making use of the following procedure. First, an inverted ratio,  $\frac{^3\text{He}}{^4\text{He}}$ , was formed and then, for the region of  $x \geq 1.15$ , the data was rebinned by combining three bins into one taking care of the error propagation. Subsequently the data

in the inverted ratio that had error bars falling below zero were moved along a truncated gaussian, such that the lower edge of the error bar was at zero. The result was then inverted to give the ratio  $^4\text{He}/^3\text{He}$  shown in Figure 3 of Ref. [6] and as the triangles in Fig. 14 below. The use of a truncated gaussian gave rise to the asymmetric error bars seen in the ratio. A limitation of this approach is that it would have to be repeated for every nucleus when forming  $\frac{\sigma^A}{\sigma^{^3\text{He}}}$ .

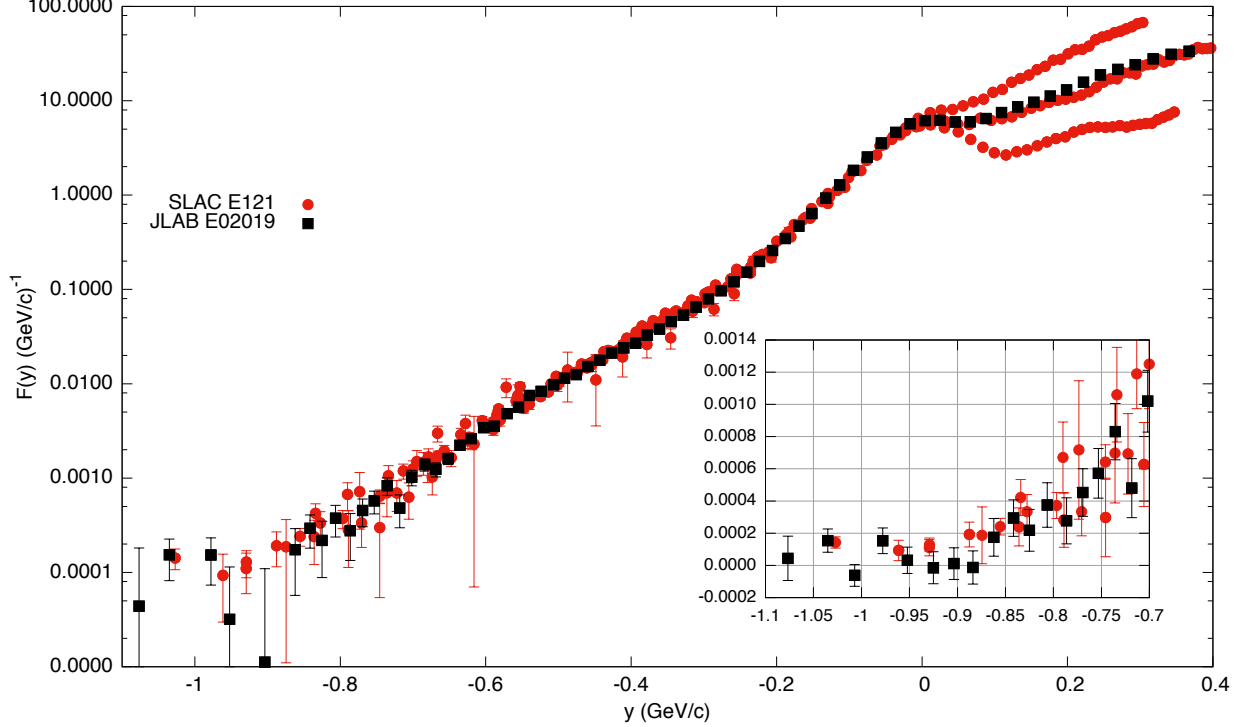


FIG. 13:  $F(y)$  plotted against  $y$  for  $^3\text{He}$  data from Ref. [6, 12, 15]. The inset shows  $F(y)$  for  $-0.7 > y > -1.1$ . This corresponds to the region of interest for 3N-SRCs,  $\alpha_{3N} \simeq 1.6$  (at  $y = -0.7$ ) to  $\alpha_{3N} \simeq 1.8$  (at  $y = -1.1$ ). The selected SLAC data shown here have  $1 < Q^2 < 4 \text{ GeV}^2/\text{c}^2$ . There is good agreement between the SLAC and Jefferson Lab data.

As an alternative to the procedure of Ref.[6] we have used the following approach[35] to avoid the problematic  $^3\text{He}$  data of Refs.[6, 49, 52] in the 3N-SRC region. We fit the y-scaling function  $F(y)$ , derived from the SLAC  $^3\text{He}$  data between  $x = 2.68$  and  $x = 2.85$  ( $1.6 \leq \alpha_{3N} \leq 1.8$ ). The fit was of the form  $F(y) = a \exp(-by)$ . We were then able to replace, point by point, the  $^3\text{He}$  cross sections from E02019 where its central value was negative or its error bar fell below zero, through the following:  $\frac{d^2\sigma}{d\Omega dE'} = \sum_{eN} \sigma_{eN} \cdot K \cdot F(y)$ .  $K$  is a kinematic factor and  $\sigma_{eN}$  is the elementary electron-nucleon cross section. The absolute



error of the E02019 data set [6, 49, 52] was kept rather than the smaller errors from the fit. The fit parameters are  $a = 0.296$  and  $b = 8.241$ . A similar approach was used in Ref. [1], where the first evidence of 2N-SRCs through cross section ratios in inclusive scattering were revealed. Subsequently those results were confirmed by precision studies[2, 3, 6] in which the heavy and light cross section data were measured in single experiment.

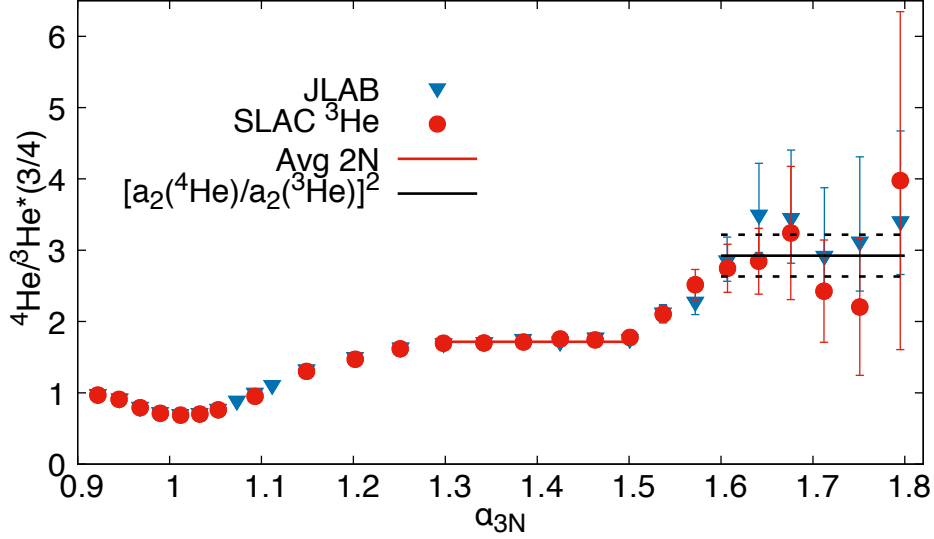


FIG. 14: The  $\alpha_{3N}$  dependence of the inclusive cross section ratios for  $^4\text{He}$  to  $^3\text{He}$ , triangles - JLAB data [6, 49], circles - ratios when using a parameterization of SLAC  $^3\text{He}$  cross sections [12, 15]. The horizontal line at  $1.3 \leq \alpha_{3N} < 1.5$  identifies the magnitude of the 2N-SRC plateau. The line for  $\alpha_{3N} > 1.6$  is Eq.(27) with a 10% error introduced to account for the systematic uncertainty in  $a_2(A, Z)$  parameters across all measurements. The data correspond to  $Q^2 \approx 2.5 \text{ GeV}^2$  at  $x = 1, \alpha_{3N} = 1$ . The figure is adapted from Ref.[35].

Fig. 14 presents the results for the cross section ratios obtained from the approaches described above; the one adopted in Ref.[6] (blue triangles) and other (red circles) in which the scaling function  $F(y)$  is used to reconstruct cross sections between  $x = 2.68$  and  $x = 2.85$  ( $1.6 \leq \alpha_{3N} \leq 1.8$ ). While both give similar results we consider the replacement of the problematic data points as a best alternative procedure of Ref [6] in part because it allows a consistent treatment of the ratios for all  $A$ .

### A. Systematic studies

We have worked to evaluate the sensitivity of the procedure above to obtain the  $\frac{^4\text{He}}{^3\text{He}}$  ratios, as measured by  $R_3^{\text{exp}}$  Eq.(19), in multiple ways. We varied the both the data sets used in the fit to  $F(y)$  and the fraction of the data in the fit range,  $-1.08 \geq y \leq -0.84$ , that is replaced. We made fits to  $F(y)$  built from 4 different data sets (1) the SLAC data only, (2) the JLAB data only, (3) both the JLAB and the SLAC data, and finally (4) the JLAB data absent its negative values. In addition, using the 4 fits to  $F(y)$ , we examined 3 variations of the fraction of the JLAB data set replaced by cross sections from the  $F(y)$  fits: all the data in the fit range; just the 6 bins in the fit range where the data or its error bar went below zero; and only the data where the cross section values were negative. We found that these 12 variations for the  $^3\text{He}$  cross sections resulted in weighted averages in the  $3\text{N}$  region that agreed easily within their error bars. See Figure 15. We show on the right hand side of Figure 15 the dependence of  $R_3^{\text{exp}}$  on the lower limit in  $\alpha_{3N}$  when taking the weighted average. As can be seen the result is not strongly dependent on  $\alpha_{3N}$  and the error bar increases due to the worsening statistics.

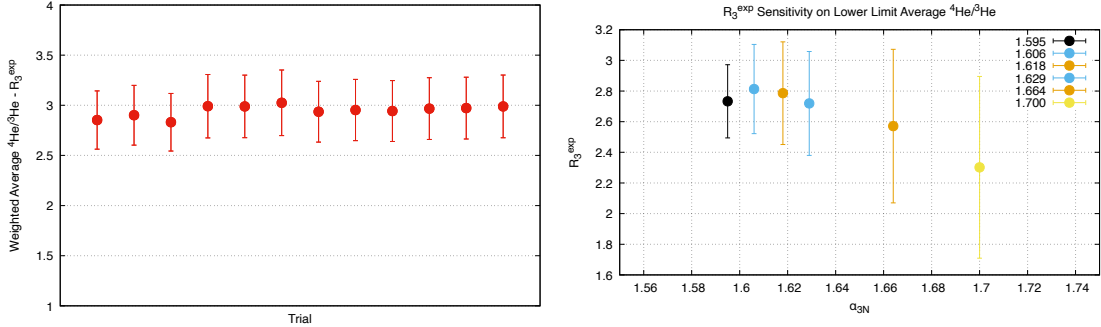


FIG. 15: Left: Sensitivity of Ratio,  $\frac{^4\text{He}}{^3\text{He}}$ , during the replacement of the anomalous  $^3\text{He}$  data procedure for 12 different trials; 4 of the data set used to form  $F(y)$  and with 3 of what fraction of the data replaced. Right: Sensitivity of Ratio  $\frac{^4\text{He}}{^3\text{He}}$  with the lower limit used when forming the weighted average with  $\alpha_{3N}$ . Sensitivity of the weighted average of  $\frac{^4\text{He}}{^3\text{He}}$  in the  $3\text{N}$  region on the lower limit of  $\alpha_{3N}$ . The results shown in Fig. 17(a) remain unchanged within errors which grow with a larger  $\alpha_{3N} > 1.6$  limit. In all cases (here and our final results) we restricted the upper limit such that  $W_{3N}$  was at least 50 MeV less than the elastic limit  $\alpha_{3N} \leq 1.75$ ,  $x \leq 2.85$  and  $y \geq -0.92$  so as to avoid, as much as possible, FSI.

Going back to Fig. 14 we notice that the plateau due to 2N-SRCs is clearly visible for  $1.3 \leq \alpha_{3N} \leq 1.5$ . In this region  $\alpha_{3N} \approx \alpha_{2N}$ , where  $\alpha_{2N}$  is the LC momentum fraction of the nucleon in the 2N-SRC. Because of this, we refer to the magnitude of this plateau as  $R_2(A, Z)$  defined in Eq.(26).

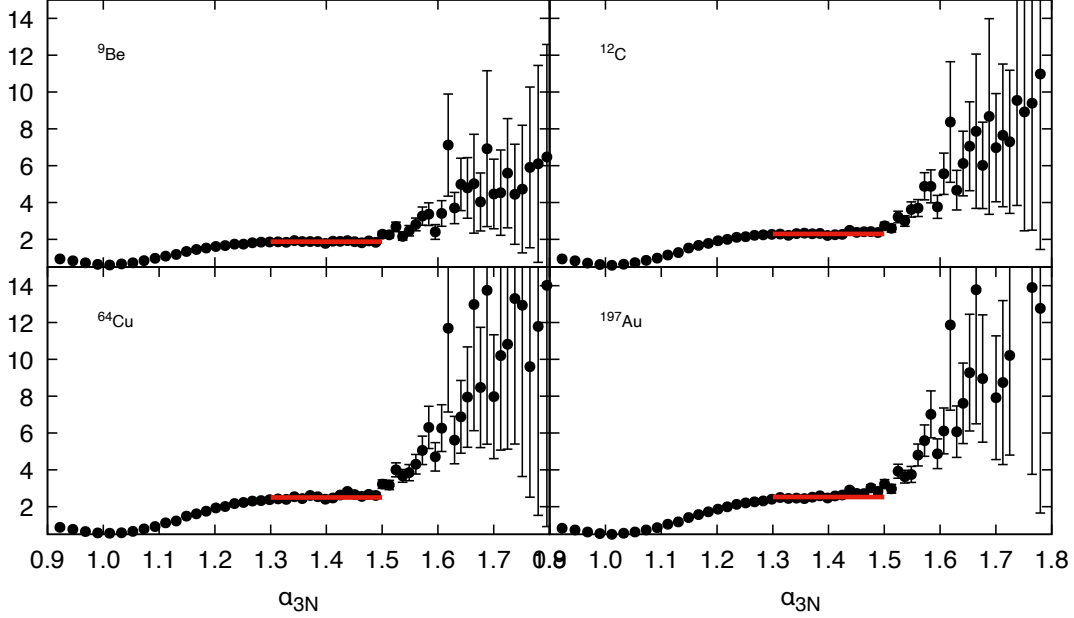


FIG. 16: Per-nucleon cross section ratios for  ${}^9\text{Be}$ ,  ${}^{12}\text{C}$ ,  ${}^{64}\text{Cu}$ ,  ${}^{197}\text{Au}$  to  ${}^3\text{He}$ . Horizontal lines indicating  $\frac{a_2(A)}{a_2({}^3\text{He})}$  in the 2N-SRC region.

The horizontal line in the region of  $1.3 \leq \alpha_{3N} \leq 1.5$  is given by the right hand side of Eq. (26), in which the values of  $a_2({}^3\text{He})$  and  $a_2(A)$  are taken from the last column of Table II in Ref. [57], an average of the SLAC, JLAB Hall C and JLAB Hall B results. The magnitude of the horizontal solid line in the region of  $1.6 \leq \alpha_{3N} \leq 1.8$ , is the prediction of  $R_{3N}(A, Z) \approx R_{2N}^2(A, Z)$  which was explained in the previous section (Eq.(27)). We assigned a 10% error to this prediction (dashed lines) related to the uncertainty of  $a_2(A, Z)$  magnitudes across different measurements.

With the same  ${}^3\text{He}$  cross sections in Fig. 16 we evaluated ratios of cross sections,  $\frac{3\sigma^A}{A\sigma^{3\text{He}}}$  for the nuclei ( ${}^4\text{He}$ ,  ${}^9\text{Be}$ ,  ${}^{12}\text{C}$ ,  ${}^{64}\text{Cu}$  and  ${}^{197}\text{Au}$ ). Despite large errors the ratios indicate visible enhancements at  $\alpha_{3N} \geq 1.6$  which are qualitatively similar to that of  $\frac{3\sigma^{4\text{He}}}{4\sigma^{3\text{He}}}$  ratios in Fig.14. Additionally in this figure, we evaluated the magnitudes of  $\frac{a_2(A)}{a_2({}^3\text{He})}$  (taken from Ref. [6]) which are indicated by horizontal lines for  $1.3 \leq \alpha_{3N} \leq 1.5$  where the plateau due

to 2N-SRCs is observed.  $\left(\frac{a_2(A)}{a_2(^3\text{He})}\right)^2$ .

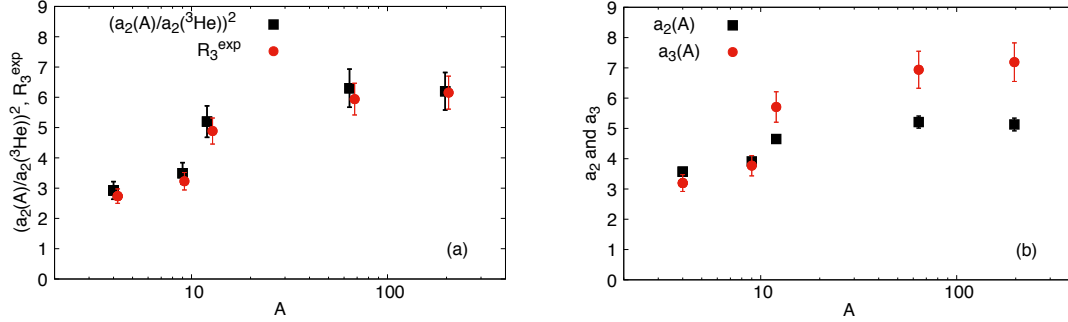


FIG. 17: (a) The  $A$  dependence of the experimental evaluation of  $R_3$  compared with the prediction of Eq. 27. (b) The  $A$  dependence of  $a_3(A, Z)$  parameter compared to  $a_2(A, Z)$  of Ref. [6].

As can be seen from these figures the data indicate the strong enhancement in the ratio,  $R_3(A)$  as soon as  $\alpha_{3N} \gtrsim 1.6$  which are in qualitative agreement with the prediction of Eq. (27). To test quantitatively the prediction of Eq. (27) in Fig. 17(a) we evaluated the weighted average of  $R_3^{\text{exp}}(A, Z)$  for  $\alpha_{3N} > 1.6$  and compared them with the magnitude of  $(\frac{a_2(A, Z)}{a_2(^3\text{He})})^2$  in which  $a_2(A, Z)$ 's are taken from Ref. [57]. In these evaluations  $^3\text{He}$  cross sections were taken from the  $F(y)$  fit to the SLAC data. Numerical data of Fig. 17 are presented also Table I. The comparison in Fig. 17(a) shows good agreement with the prediction of Eq. (27) for the full range of nuclei. We investigated the sensitivity of the weighted average of  $R_3(A, Z)$  on the lower limit of  $\alpha_{3N}$  (before rebinning) and found that the results shown in Fig. 17(a) remain unchanged within errors which grow with a larger  $\alpha_{3N} > 1.6$  cut.

The agreement presented in Fig. 17(a) represents the strongest evidence yet for the presence of 3N-SRCs. If it is indeed due to the onset of 3N-SRCs then one can use the measured  $R_3^{\text{exp}}$  ratios and Eq. (21) to extract the  $a_3(A, Z)$  parameters characterizing the 3N - SRC probabilities in the nuclear ground state. The estimates of  $a_3(A, Z)$  and comparisons with  $a_2(A, Z)$  are given in Fig. 17(b) (see also Table I). These comparisons show a faster rise for  $a_3(A, Z)$  with  $A$ , consistent with the expectation of the increased sensitivity of 3N-SRCs to the local nuclear density [32]. If this result is verified in the future with better quality data and a wider range of nuclei then the evaluation of the parameter  $a_3(A, Z)$  as a function of nuclear density and proton/neutron asymmetry together with  $a_2(A, Z)$  can provide an important theoretical input for the exploration of the dynamics of super dense nuclear matter

(see e.g. [58]).

TABLE I: Numerical values  $a_2$ [57],  $R_2$  (Eq. 26),  $R_3^{\text{exp}}$  (the weighted average in the 3N region) and  $a_3$  calculated from Eq. 21.

A	$a_2$	$R_2$	$R_3^{\text{exp}}$	$a_3$
3	$2.13 \pm 0.04$	1	NA	NA
4	$3.57 \pm 0.09$	$1.68 \pm 0.03$	$2.74 \pm 0.24$	$3.20 \pm 0.28$
9	$3.91 \pm 0.12$	$1.84 \pm 0.04$	$3.23 \pm 0.29$	$3.77 \pm 0.34$
12	$4.65 \pm 0.14$	$2.18 \pm 0.04$	$4.89 \pm 0.43$	$5.71 \pm 0.50$
64	$5.21 \pm 0.20$	$2.45 \pm 0.04$	$5.94 \pm 0.52$	$6.94 \pm 0.77$
197	$5.13 \pm 0.21$	$2.41 \pm 0.05$	$6.15 \pm 0.55$	$7.18 \pm 0.64$

## VII. SUMMARY AND OUTLOOK

We determined the kinematic conditions for isolating 3N SRCs in inclusive  $A(e, e')X$  reaction at large  $x$ . Based on the analysis of short range structure of  $^3\text{He}$  nuclei we expect that the dominant mechanism of 3N SRCs in inclusive processes is due to three-nucleon correlations, in which one fast nucleon is balanced by two spectator nucleons with rather small invariant mass,  $2m_N \leq m_S \lesssim 1.9$  GeV. Momenta of all three nucleons, however, exceed the characteristic Fermi momentum of the nucleus  $k_F \sim 250$  MeV/c. We referred such correlations as type 3N-I SRCs.

We explain that due to the specific nature of the high momentum components of the nuclear wave functions, the momentum of the fast nucleon is not the optimal variable for the analysis since it does not allow the separation of 2N and 3N SRCs. In this respect the light-cone momentum fraction of 3N-SRC carried by the interacting nucleon,  $\alpha_{3N}$  is more suitable and existing phenomenology indicates that the onset of the 3N-SRC dominance is expected at  $\alpha_{3N} > 1.6$ . We derived the expression for  $\alpha_{3N}$  for inclusive  $A(e, e')X$  processes and demonstrated that the  $\alpha_{3N} \gtrsim 1.6$  condition puts a strong constraint on  $Q^2$  of the reaction - requiring  $Q^2 \gtrsim 3$  GeV<sup>2</sup>. Under these conditions we expect that the dominance of 3N-SRCs will lead to a plateau for per-nucleon inclusive cross section ratios of heavy to light nuclei. This will be in addition to the plateau observed in the 2N-SRC region.

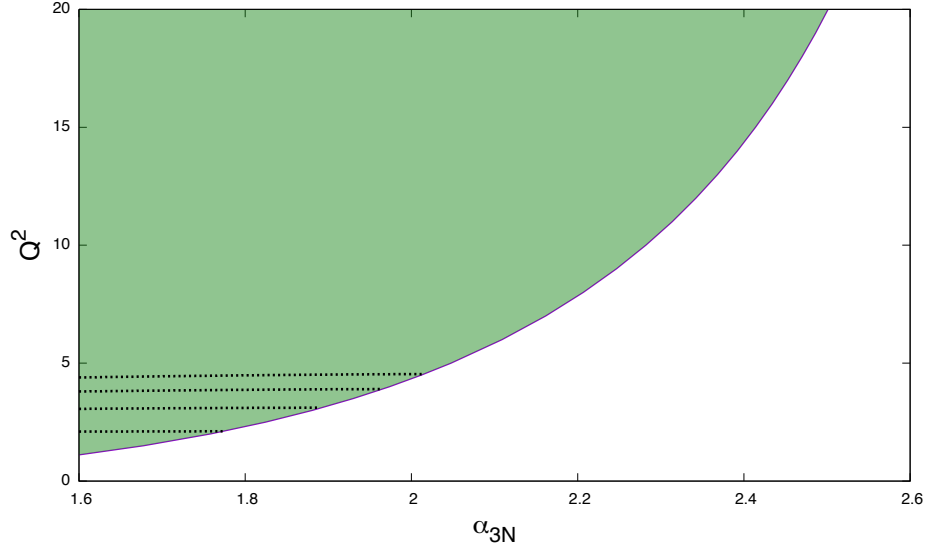


FIG. 18: The  $Q^2$  range necessary in order to isolate 3N-SRCs. Also shown is the kinematic extent of an upcoming 12 GeV experiment [56].

Furthermore, based on the  $pn$  dominance in 2N-SRCs we predict that 3N-SRCs are generated through two successive  $pn$  short range interactions. Within such scenario we derived a quadratic relation between per nucleon ratios of nuclear and  ${}^3\text{He}$  inclusive cross sections measured in the 2N- ( $R_2$ ) and 3N- ( $R_3$ ) SRC regions:  $R_3 \approx R_2^2$ .

We analyzed the existing inclusive data under the above conditions and found an indication for the onset of the plateau at  $\alpha_{3N} > 1.6$ . It is very intriguing that the magnitude of the plateau,  $R_3$  is in agreement with predicted  $R_3 \approx R_2^2 \approx (\frac{a_2(A)}{a_2({}^3\text{He})})^2$  dependence. This agreement allowed us to extract per nucleon probabilities,  $a_3(A, Z)$  of finding 3N-SRCs in nuclei-A relative to the  ${}^3\text{He}$  nucleus.

The forthcoming experiments at Jefferson Lab will be able to significantly improve current experimental situation. One important condition is that such experiments will be able to cover a larger  $Q^2$  region. As Fig. 18 shows an increase of  $Q^2$  will significantly widen the range of the  $\alpha_{3N}$  accessible by the experiment. It is worth mentioning that at  $Q^2 \gtrsim 5 \text{ (GeV/c)}^2$  one will be able to cross to the  $\alpha_{3N} \geq 2$  region where one expects maximal contribution due to 3N SRCs.

It is with anticipation that we await the running and analysis of Jefferson Lab's E1206-105[56] experiment which has multiple goals: to measure cross sections 1) from light nuclei to compare to ab-initio calculations and to study FSI, 2) from nuclei at low and moderate  $Q^2$

with a range of  $p - n$  asymmetries in order to look for isospin dependence in the per-nucleon ratios, 3) at moderate  $Q^2$  and large  $x$  to search for definitive evidence to 3N SRCs and finally 4) at very large  $Q^2$  to look for the transition from quasielastic to deep inelastic scattering from nuclei as part of an effort to extract nuclear parton distribution functions at  $x > 1$ . The drawn lines in Fig. 18 indicate the tentative range in  $Q^2$  and  $\alpha_{3N}$  which will be part of the goal of this experiment in studying 3N SRCs.

Finally, further studies of semi-inclusive processes using different probes are necessary. For example, one could look for final states containing three nucleons in the kinematics corresponding to the scattering off type 3N-II SRCs. In particular, it would be instructive to compare production of 3N system in different isospin states: 3 protons, where contribution of the repulsive core is enhanced, and 2p+n state in which the attraction dominates.

**Acknowledgments:** This work was supported in part by the DOE Office of Science, Office of Nuclear Physics, contracts DE-FG02-96ER40950 (DBD), DE-FG02-93ER40771 (MIS), and DE-FG02-01ER41172 (MSS).

- 
- [1] L. L. Frankfurt, M. I. Strikman, D. B. Day and M. Sargsian, Phys. Rev. C **48**, 2451 (1993).
  - [2] K. S. Egiyan *et al.* [CLAS Collaboration], Phys. Rev. C **68**, 014313 (2003).
  - [3] K. S. Egiyan *et al.* [CLAS Collaboration], Phys. Rev. Lett. **96**, 082501 (2006).
  - [4] R. Shneor *et al.* [Jefferson Lab Hall A Collaboration], Phys. Rev. Lett. **99**, 072501 (2007).
  - [5] R. Subedi, R. Shneor, P. Monaghan, B. D. Anderson, K. Aniol, J. Annand, J. Arrington and H. Benaoum *et al.*, Science **320**, 1476 (2008).
  - [6] N. Fomin, J. Arrington, R. Asaturyan, F. Benmokhtar, W. Boeglin, P. Bosted, A. Bruell and M. H. S. Bukhari *et al.*, Phys. Rev. Lett. **108**, 092502 (2012).
  - [7] J. Arrington, D. W. Higinbotham, G. Rosner and M. Sargsian, Prog. Part. Nucl. Phys. **67**, 898 (2012).
  - [8] J. L. S. Aclander *et al.*, Phys. Lett. B **453**, 211 (1999).
  - [9] A. Tang *et al.*, Phys. Rev. Lett. **90**, 042301 (2003).
  - [10] S. Rock *et al.*, Phys. Rev. Lett. **49**, 1139 (1982).
  - [11] R. G. Arnold *et al.*, Phys. Rev. Lett. **61**, 806 (1988).
  - [12] D. Day *et al.*, Phys. Rev. Lett. **43**, 1143 (1979).

- [13] D. B. Day *et al.*, Phys. Rev. Lett. **59**, 427 (1987).
- [14] W. P. Schutz *et al.*, Phys. Rev. Lett. **38**, 259 (1977).
- [15] S. Rock *et al.*, Phys. Rev. C **26**, 1592 (1982).
- [16] I. Yaron, J. Alster, L. Frankfurt, E. Piasetzky, M. Sargsian and M. Strikman, Phys. Rev. C **66**, 024601 (2002).
- [17] L. L. Frankfurt and M. I. Strikman, Phys. Rept. **76**, 215 (1981).
- [18] E. Piasetzky, M. Sargsian, L. Frankfurt, M. Strikman and J. W. Watson, Phys. Rev. Lett. **97**, 162504 (2006).
- [19] M. M. Sargsian, T. V. Abrahamyan, M. I. Strikman and L. L. Frankfurt, Phys. Rev. C **71**, 044615 (2005).
- [20] R. Schiavilla, R. B. Wiringa, S. C. Pieper and J. Carlson, Phys. Rev. Lett. **98**, 132501 (2007).
- [21] M. M. Sargsian, Phys. Rev. C **89**, no. 3, 034305 (2014) [arXiv:1210.3280 [nucl-th]].
- [22] O. Hen, M. Sargsian, L. B. Weinstein, E. Piasetzky, H. Hakobyan, D. W. Higinbotham, M. Braverman and W. K. Brooks *et al.*, Science **346**, 614 (2014).
- [23] M. Duer *et al.* [CLAS], Phys. Rev. Lett. **122**, no.17, 172502 (2019) doi:10.1103/PhysRevLett.122.172502 [arXiv:1810.05343 [nucl-ex]].
- [24] M. Duer *et al.* [CLAS], Nature **560**, no.7720, 617-621 (2018) doi:10.1038/s41586-018-0400-z
- [25] C. Ciofi degli Atti, S. Simula, L. L. Frankfurt and M. I. Strikman, Phys. Rev. C **44**, R7 (1991).
- [26] C. Ciofi degli Atti and S. Simula, Phys. Rev. C **53**, 1689 (1996).
- [27] J. Ryckebusch, W. Cosyn and M. Vanhalst, J. Phys. G **42**, no. 5, 055104 (2015).
- [28] O. Artiles and M. M. Sargsian, Phys. Rev. C **94**, no. 6, 064318 (2016).
- [29] C. Ciofi degli Atti, C. B. Mezzetti and H. Morita, Phys. Rev. C **95**, no. 4, 044327 (2017).
- [30] H. Heiselberg and V. Pandharipande, Ann. Rev. Nucl. Part. Sci. **50**, 481-524 (2000) doi:10.1146/annurev.nucl.50.1.481 [arXiv:astro-ph/0003276 [astro-ph]].
- [31] N. Fomin, D. Higinbotham, M. Sargsian and P. Solvignon, Ann. Rev. Nucl. Part. Sci. **67**, 129 (2017).
- [32] L. Frankfurt, M. Sargsian and M. Strikman, Int. J. Mod. Phys. A **23**, 2991 (2008).
- [33] Z. Ye *et al.* [Hall A], Phys. Rev. C **97** (2018) no.6, 065204 doi:10.1103/PhysRevC.97.065204 [arXiv:1712.07009 [nucl-ex]].
- [34] D. W. Higinbotham and O. Hen, Phys. Rev. Lett. **114**, no. 16, 169201 (2015).
- [35] M. M. Sargsian, D. B. Day, L. L. Frankfurt and M. I. Strikman, Phys. Rev. C **100**, no.4,



- 044320 (2019) doi:10.1103/PhysRevC.100.044320 [arXiv:1910.14663 [nucl-th]].
- [36] N. Fomin. “Inclusive Scattering from Nuclei in the Quasielastic Region at Large Momentum Transfer”. PhD thesis, University of Virginia, 2007. arXiv:0812.2144.
  - [37] L. L. Frankfurt and M. I. Strikman, Phys. Rept. **160**, 235 (1988).
  - [38] M. M. Sargsian, Int. J. Mod. Phys. E **10**, 405 (2001).
  - [39] L. L. Frankfurt, M. M. Sargsian and M. I. Strikman, Phys. Rev. C **56**, 1124 (1997).
  - [40] M. M. Sargsian, T. V. Abrahamyan, M. I. Strikman and L. L. Frankfurt, Phys. Rev. C **71**, 044614 (2005).
  - [41] A. Nogga, A. Kievsky, H. Kamada, W. Gloeckle, L. E. Marcucci, S. Rosati and M. Viviani, Phys. Rev. C **67**, 034004 (2003).
  - [42] A. J. Freese, M. M. Sargsian and M. I. Strikman, Eur. Phys. J. C **75**, no. 11, 534 (2015).
  - [43] R. B. Wiringa, R. Schiavilla, S. C. Pieper and J. Carlson, Phys. Rev. C **89**, no. 2, 024305 (2014).
  - [44] W. Boeglin and M. Sargsian, Int. J. Mod. Phys. E **24**, no. 03, 1530003 (2015).
  - [45] W. Cosyn and M. Sargsian, Int. J. Mod. Phys. E **26**, no. 09, 1730004 (2017).
  - [46] W. Cosyn, W. Melnitchouk and M. Sargsian, Phys. Rev. C **89**, no. 1, 014612 (2014).
  - [47] M. M. Sargsian, Phys. Rev. C **82**, 014612 (2010).
  - [48] D. B. Day *et al.*, Phys. Rev. C **48**, 1849 (1993).
  - [49] N. Fomin *et al.*, Phys. Rev. Lett. **105**, 212502 (2010).
  - [50] N. Fomin, PhD thesis, University of Virginia, 2007, arXiv:0812.2144.
  - [51] N. Fomin, AIP Conf. Proc. **947**, 174 (2007).
  - [52] John Arrington, Donal Day, Allison Lung, and Brad Filippone (spokespersons). Inclusive Scattering from Nuclei at  $x > 1$  and High  $Q^2$  with a 6 GeV Beam. Jefferson Lab Experiment No. E-02-019, unpublished, 2002.
  - [53] N Fomin, private communication.
  - [54] D. B. Day, J. S. McCarthy, T. W. Donnelly and I. Sick, Ann. Rev. Nucl. Part. Sci. **40**, 357 (1990).
  - [55] I. Sick, D. Day and J. S. McCarthy, Phys. Rev. Lett. **45**, 871 (1980).
  - [56] John Arrington and Donal Day (spokespersons) Inclusive scattering from nuclei at  $x > 1$  in the quasielastic and deeply inelastic regimes. Jefferson Lab Experiment No. E12-06-105, unpublished, 2006.

- [57] J. Arrington, A. Daniel, D. Day, N. Fomin, D. Gaskell, and P. Solvignon, Phys. Rev. C **86**, 065204 (2012).
- [58] D. Ding, A. Rios, H. Dussan, W. H. Dickhoff, S. J. Witte, A. Polls, A. Carbone, Phys. Rev. C **94**, 025802 (2016).
- [59] This variable has a equivalence with Bjorken  $x_{Bj}$  that describes the light-cone momentum fraction of the nucleon carried by a parton.